

**IFT**

**IOFFE FUSION TECHNOLOGY**

*26, Politekhnicheskaja Street, St. Petersburg 194021, Russia*

I.V.Basargin, A.P.Bedin

**ANOMALOUS PROPERTIES OF SHOCKS  
IN PLASMA AND REACTING GASES**

EOARD Contract No. F61708-97-W0015  
(SPC-97-4001)

**DISTRIBUTION STATEMENT A**

Approved for public release  
Distribution unlimited

St.Petersburg  
1998

19980227 026

DTIC QUALITY INSPECTED 3

**REPORT DOCUMENTATION PAGE**

Form Approved OMB No. 0704-0188

Public reporting burden for this collection of information is estimated to average 1 hour per response, including the time for reviewing instructions, searching existing data sources, gathering and maintaining the data needed, and completing and reviewing the collection of information. Send comments regarding this burden estimate or any other aspect of this collection of information, including suggestions for reducing this burden to Washington Headquarters Services, Directorate for Information Operations and Reports, 1215 Jefferson Davis Highway, Suite 1204, Arlington, VA 22202-4302, and to the Office of Management and Budget, Paperwork Reduction Project (0704-0188), Washington, DC 20503.

1. AGENCY USE ONLY (Leave blank)		2. REPORT DATE  1998	3. REPORT TYPE AND DATES COVERED  Final Report	
4. TITLE AND SUBTITLE  Anomalous Properties of Shocks in Plasma and Reacting Gases			5. FUNDING NUMBERS  F6170897W0015	
6. AUTHOR(S)  Dr. Albert Bedine				
7. PERFORMING ORGANIZATION NAME(S) AND ADDRESS(ES)  Ioffe Physico-Technical Institute of Russian Academy of Sciences Polytechnicheskaya str., 26 St. Petersburg 194221 Russia			8. PERFORMING ORGANIZATION REPORT NUMBER  N/A	
9. SPONSORING/MONITORING AGENCY NAME(S) AND ADDRESS(ES)  EOARD PSC 802 BOX 14 FPO 09499-0200			10. SPONSORING/MONITORING AGENCY REPORT NUMBER  SPC 97-4001	
11. SUPPLEMENTARY NOTES				
12a. DISTRIBUTION/AVAILABILITY STATEMENT  Approved for public release; distribution is unlimited.			12b. DISTRIBUTION CODE  A	
13. ABSTRACT (Maximum 200 words)  This report results from a contract tasking Ioffe Physico-Technical Institute of Russian Academy of Sciences as follows: The contractor will investigate anomalous properties of shocks as per his July 94 and June 96 proposals.				
14. SUBJECT TERMS  Fluid Dynamics			15. NUMBER OF PAGES  55	
			16. PRICE CODE N/A	
17. SECURITY CLASSIFICATION OF REPORT  UNCLASSIFIED	18. SECURITY CLASSIFICATION OF THIS PAGE  UNCLASSIFIED	19. SECURITY CLASSIFICATION OF ABSTRACT  UNCLASSIFIED	20. LIMITATION OF ABSTRACT  UL	

NSN 7540-01-280-5500

Standard Form 298 (Rev. 2-89)  
Prescribed by ANSI Std. Z39-18  
298-102

# ANOMALOUS PROPERTIES OF SHOCKS IN PLASMA AND REACTING GASES

EOARD Contract No.F61708-97-W0015(SPC-97-4001)

Principal Investigator: Dr. A.P.Bedin

Ioffe Physico-Technical Institute of Russian Academy of Sciences ( Ioffe Fusion Technology)

St.-Petersburg

I.V.Basargin, A.P.Bedin

## Summary / Overview

The first ballistic range of the plasmogasdynamics laboratory of Ioffe Physico-Technical Institute has been created in 1953. It was intended for investigations of the drag and the flow around bodies in the free flight at sub-, super- and hypersonic velocities [1]. At present the experimental base of the laboratory consists of two hypersonic ballistic ranges and the shock tube of the electrical discharge type [2-4]. The installations are used to investigate aerodynamic characteristics of different bodies and the flow around the bodies in various media; properties of shock waves propagating in different gases and plasma; the hypersonic wake behind flying bodies; the shock waves-moving and motionless bodies interaction; the interaction of flying bodies with the heat, plasma and blast heterogeneities as well with motionless obstacles and etc.

In the report we adduce the brief description of the experimental installations of the laboratory and discuss the results of studying the anomalous phenomena arising under the shock waves and bodies movement in reacting gases and in low temperature gas discharge plasma.

When moving shock waves and bodies in reacting gases at the regimes of the anomalous relaxation, it is appeared the instability of shock waves, the flow behind the shock waves and the inviscid wake behind flying bodies become turbulent, it is changed the drag of a body and the heat flux on its surface, it is observed the anomalous emission and so on.

While moving shock waves and bodies in low temperature gas discharge plasma, it is expended the velocities range with the subsonic regime of the flow around bodies, it is changed the drag, the pressure distribution and the heat flux, the velocity of the shock waves propagation increases, the shock wave structure changes and so forth.

All the phenomena are caused by nonequilibrium physico-chemical processes in plasma or in reacting gases when shock or sonic waves are propagating in these media. In this report it is analyzed all the complex of anomalous phenomena which

occur when moving shock waves and bodies in reacting gases or in plasma and is discussed the nature of these phenomena.

## Technical Discussion

### 1. Experimental Installations

In this section it is adduced the description of the experimental installations of the plasmogasdynamic laboratory of Ioffe Physico-Technical Institute [2-4].

The scheme of one of them (the ballistic range BU-88 FTI RAN [2]) is shown in Fig.1. This installation is destined for studying aerodynamic characteristics and the flow around bodies in various gases and plasma under sub-, super- and hypersonic velocities of a flight. As it is seen on Fig.1 the installation consists of the powder gun ( the muzzle velocity  $V \leq 2,5$  km/s, the calibres of test models  $d=10-30\text{mm}$ ), the system of cutting off parts of the case from the flying model (the case protects the model from the damage under its movement through the barrel), the pressurized chamber ( the length -11m, the inner diameter -0,3m), the optical and electronic apparatus and the bullet collector.

Experiments are carried out in the following way: the test model is mounted in the barrel at the required angle of attack by means of the composite case (the composite design of the case facilitates the separation its parts from the fired model). The barrel is evacuated up to the forvacuum and then the model is shot.

The shot model is separated from details of the case and is flying into the pressurized chamber which is filled up working gas. In the flight the test model usually oscillates relatively to the zero or balance angle of attack. The entrance velocity of the model in the pressurized chamber can change with the powder weight from 0.15km/s to 2.5km/s. The working range of the pressure is  $50-3 \cdot 10^5$  Pa. The experiments are conducted in any gases, mixture of gases and plasma. And so in experiments it is reproduced the numbers  $M$  and  $Re$  near to the full-scale ones (see Fig.2). In case in experiments it is used gases having the sonic velocity less than the freon-12 one, numbers  $M$  up to 25 can be obtained at the installation.

Having flown in the pressurized chamber the test model is being photographed successively by the shadow or Toeplers methods in two mutual perpendicular directions in 17 points of the track. The scheme of photographing is shown in Fig.3.

Impulse light sources 1 ( the duration of the luminescence  $\sim 40\text{ns}$ ) are placed in foci of objectives 2 ( we use the objectives T-11M with the focal distance 1200mm, the relative aperture 1:9 and Telemar 7M with 1000mm, 1:7). Owing to it we attain the parallelism of the light beams which cross the working zone of the installation (the zone of the registration of the flying model). The working zone is enlightened in two directions through the glass windows 4 of pressurized chamber 7. There are the coordinate systems 5 on the external side of windows, they are the crossed tight steel strings. The turn -mirrors 3 are intended for the diminution of the cross-gabarit of the installation. The objective 8 placed the two focal distance from

the pressurized chamber axis images the flying model in the plane which is disposed the two local distance from this objective. In this plane it is placed a photocassette 10 if it is necessary to obtain the schlieren photograph. There is an optical knife 9 in the focus of the objective 8 serving for the increase of sensibility of the schlieren system. The ordinary shadow photographs are received if the cassettes are placed in the position 6. The scale of the photographs is 1:1 in both cases.

The flying model is photographed automatically by means of the synchronizing apparatus devised in our institute [6,8]. Flying in the pressurized chamber the model fired by the gun is crossing narrow bunches of the light emitted by the slit sources of the light  $i_n$  (Fig.1). It is caused the change of the illuminance of photocathodes of photomultipliers (PM)  $f_n$  which are disposed at the opposite side of the installation. As a result every PM generates the electrical signal which goes to the conformable block of the synchronizing apparatus  $B_n$  where it is amplified, is formed and is delayed for a time which is necessary the model to fly from PM to the center of a visual field of the objective. The delayed signal goes to the spark generator, the last produces a short light pulse exposing a photofilm. Electronic chronographs placed at the control panel are measuring the time between the moments of exposing. A totality of photographs obtained in each experiment together with data of measurements of geometric parameters of test model and its mass, of the pressure and the temperature of the working gas and etc. is the primary experimental information which is necessary for determining aerodynamic characteristics, for studying the flow around the model and physico-chemical processes before and behind shock waves and hypersonic wakes.

In the ballistic experiment aerodynamic characteristics are determined from data of measurements of photographs and of model parameters by methods which are founded on using the differential relations between aerodynamic coefficients and parameters of trajectory of the test model. These relations are fixed by the general equations of the motion. All the methods are reduced essentially to determining linear and angular velocities and accelerations from experimental data and it requires differentiation (including double one) of experimental dependencies and to the following calculation of aerodynamic coefficients with using the equations of the motion [2,9,10]. The differentiation of experimental dependencies (especially double one) is accompanied by the increase of derivatives errors. As a rule it results that the mistakes of the calculation of second derivatives of angular and linear coordinates with respect to the time or the longitudinal coordinate become the main part of the mean-square errors of aerodynamic characteristics. The mistakes of the calculation of derivatives are directly proportional to the mean square errors of the measurement of linear and angular coordinates. Therefore the accuracy of the determination of aerodynamic characteristics of bodies in free flight depends in the main on the accuracy of measurements of their coordinates. The last is affected by:

- 1) the quality and the feature of optical system of the installation;

- 2) characteristics of impulse light sources used for exposing a photofilm and also characteristics of itself film;
- 3) the quality of adjustment of optical systems of installation;
- 4) the quality of fitting local systems of coordinates to the laboratory coordinates system.

Two last factors can make the considerable contribution to the value of errors of the measurement of coordinates. And so we are paying much attention to the adjustment of the optical equipment of the installation BU-88. Our methods of the adjustment of the optical systems of the ballistic range [2,11] allow to measure the linear coordinates of the flying model with the accuracy  $0.02\text{mm} < \sigma_{x,y} < 0.15$  and the angular coordinates with accuracy  $0.03^\circ < \sigma_{\theta,\psi} < 0.3^\circ$ . The superior limit corresponds with the case when the measurement of coordinates is carried out by shadow photographs and the inferior limit - by Toepler ones. It allows to define the aerodynamic characteristics by the ballistic range BU-88 with the accuracy  $\sigma_{C_x} = \sigma_{C_y} = 10 \sigma_{C_m} = 0.005-0.015$  [2].

The ballistic installation GBU [3] is intended to the investigations of physico-chemical processes before and behind shock waves and into hypersonic wakes, of heat physic processes, of the interaction of hypersonic bodies with motionless obstacle and so on. In many respects its construction is like the one of the BU-88 installation: GBU consists of the gun, the system of cutting off the case from the model, the pressurized chamber with the optical, electronic and other apparatus and the bullet assembler. But there are the differences between the ballistic ranges. So GBU in contrast to BU-88 has been equipped with both the powder gun ( $V \leq 2.5 \text{ km/s}$ ) and the gasdynamic one ( $V \leq 6.4 \text{ km/s}$ ). Besides the equipments of the installations are different as it is seen on Fig.1 and Fig.4 which demonstrate the schemes of the BU-88 and GBU ballistic ranges.

The electrical discharge shock tube of the plasmogasdynamic laboratory [4] serves for researches of physico-gasdynamic properties of shock waves propagating in plasma or in different gases. It consists of the electromagnetic shock tube 2 (Fig.5) and the discharge chamber 4 which is created the glow discharge of the continuous current in. The shock waves of the blast type are generated by the power impulse discharge between coaxial electrodes joined with the feeding block of the discharger. The velocity of the propagation of shock waves in the tube (up to  $1600\text{m/s}$ ) is registered by means of the two-channel schlieren-system 3. Each channel consists of the fixed light source, of the lenses, of the optical slot, of the optical knife and photopick-ups. A receiver, air evacuation valves, intake valves and systems of the pressure control are placed at the pressurized chamber 5. The pick-ups (thermocouples, electrical probes, piezopick-ups and etc.) are fastened to the bar 6, which can be shifted along its axis at the great distance. The shift of the bar is carried out by means of the step motor which is operated by the signal coming from the control panel. The experiment is conducted cyclically (the interval between two cycles is  $\sim 2\text{min}$ ). The start of the shock tube, the registration of shock

waves, all the measurements and the treatment of experiments data are carried out automatically with the help of the CAMAK system and of the personal computer.

Thus the experimental base of the plasmogasdynamic laboratory permits to research aerodynamic characteristics and the flow around different bodies, heat physic processes and the propagation of shock waves in various gas media and plasma. Some results of these researches are described below.

## 2. Anomalous Phenomena under Moving Shock Waves and Bodies in Reacting Gases

In this section of the report we describe the results of theoretical and experimental researches of anomalous phenomena arising under a motion of shock waves and supersonic bodies in reacting gases.

The first photographs of the free flight sphere in freon-12 demonstrating some of these anomalies (perturbances of the shock wave front and the inviscid wake) were published in the Hilton monograph [12]. Examples of similar photographs obtained by us at regimes of anomalous flow around a blunted body in freon-12 are represented in Fig. 6.

Some time later photos of sphere flying in freon -12,14,114 which demonstrate the bow shock wave and wake disturbances were obtained by W. Maslennikov, G. Mishin, G. Tumakajev in Ioffe Physico-Technical Institute of Russian Academy of Sciences.

As a result of these experiments it was ascertained that the appearance of flow disturbances is accompanied by the dissociation of freons.

In 1976 the instability of shock waves (perturbances of the shock wave front) was discovered in  $\text{CO}_2$  ( $p = 7.6$  Torr, critical velocities  $V_c = 3.7, 5.3, 6.2$  km/s) and in Ar ( $p \approx 1$  Torr,  $V_c \approx 11$  km/s) [13]. Besides, in these experiments conducted in a shock tube it was found out that the shock wave front remained smooth when moving the shock wave with the velocity  $V < V_c$ . The authors ascertained that regimes of the instability of shock waves discovered by them did not satisfy D'jakov's criteria of the instability of shock waves [14]. Besides, they noticed, that the adiabat has Z-form by unsteady regimes.

Perturbances of the relaxation zone in Ar ( $p \approx 5$  Torr,  $V_c \sim 4.5$  km/s) were discovered in [15]. The perturbances were decreased essentially by the hydrogen impurity.

The strong shock waves instability in series of gases (Ar,  $\text{CO}_2$ ,  $\text{O}_2$ ,  $\text{H}_2$ , He, CO, air, water steam) was detected in shock tube experiments carried out under the pressure  $p < 5$  Torr [16]. But all the researches were fragmentary and did not explain the nature of the shock waves instability.

We observe this phenomenon in freons in the sixties while researching aerodynamic characteristics and a flow around blunted bodies in various gases.

These researches are conducted in connection with a creation of cosmic probes that was intended for the entry in the atmosphere of planets of the solar system. The bow shock waves instability accompanied with the turbulization of the inviscid wake behind the flying model which arises with attaining of critical numbers  $M$  has hindered conducting these investigations and so we have learned to fight with it and then began to study this phenomenon. In free flight experiments [17-19] it was ascertained that characteristics of the matter of test models (metals, plastics) and their surface (roughness, sound vibrations) did not influence on beginning the shock wave instability. At the same time these experiments demonstrated that the rise of the instability and its development are affected by the kind of a gas, the number  $M$ , the pressure and the form of a model. It was found out that the instability of the shock wave rises when the temperature of a gas and the pressure behind the shock reach values which are necessary to begin the weak dissociation of freons. The evaluation of the energy of turbulent fluctuations in the inviscid wake behind free flight models in freons gave the value commensurable with the vibrational energy in the blunt body stagnation point [20,21]. All the data permit to conclude that there is a mechanism of transformation of the energy of high excited inner degrees of freedom laid in a stock at the shock wave front in the kinetic energy. This mechanism brings to the intensification of small disturbances of gasdynamic parameters and consequently to the instability of the shock wave [17]. Common concepts of such mechanism were formulated in Ref.[22]. In this article it was suggested criteria of the shock wave instability and was discussed one of the possible kinetic mechanisms - the dissociation of excited molecules with heating products of a reaction (it was considered an occasion of molecules with one active level).

The series of the following articles [23-25] dealt with results of the searches of regimes of the instability of shock waves in different gases, of the elaboration of the instability criteria and of the study of anomalous phenomena accompanying the shock waves instability. It is appropriate to note that in shock tube experiments [13,15,16,24,25] it was registered only separate regimes of the shock wave instability (though in different gases). At that time in free flight experiments it was determined not only the fields of the existence (in  $p$ ,  $M$  variables) of the instability of flow but also the position of neutral curves at the  $p$  -  $M$  diagram for different models of various diameters in some freons (see Ref.[23]). The neutral curves  $p_c = p_c(M)$  separate the stable from unsteady flow at the  $p$  -  $M$  diagram. One of such curves is shown in Fig.7. According to data of free flight experiments the location of neutral curves at the  $p$  -  $M$  diagram depends on the sort of reacting gas, on the form and dimensions of a body.

The analysis of all the data [12-25] as well of new results concerning perturbances of shock waves, the emission, the drag, the heat flux and so on allowed to formulate fundamental features of the phenomenon of the anomalous relaxation (AR) in shock waves in gases [26]. The AR phenomenon is a nonequilibrium effect and involves strong transfer of the excitation energy into kinetic one. AR manifests itself in the series of effects: perturbation and destruction



of the shock wave front, increase of body drag, increase of heat release behind the front, random perturbations of the relaxation zone, nonmonotonous change of the gasdynamic parameters with the distance from the front, anomalous emission.

Theoretical bases of the AR phenomenon founded in Refs.[22,23,26] were supplemented and developed in Refs.[27,28]. As a result of these investigations it was suggested a simple criterion of determining regimes of AR :

$$mV^2 = \alpha \varepsilon_a, \quad (1)$$

where  $m$  is mass of a gas particle before the shock wave,  $\varepsilon_a$  is the energy of the excited particle,  $\alpha = \alpha(\rho_1, T_1)$  is the coefficient depending on flow conditions before the shock wave,  $\rho_1$ ,  $T_1$  are the density and the temperature of the undisturbed flow. This relation can be written in the other form :

$$\mu V_c^2 = 96 \alpha \varepsilon_a. \quad (2)$$

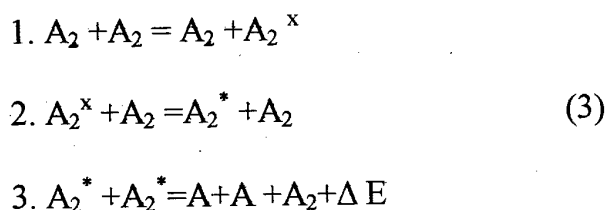
Here  $\mu$  is the molecular weight,  $V_c$  is the critical velocity of arising the shock wave instability (in km/s),  $\varepsilon_a$  is in eV.

Estimates  $V_c$  in different media conducted with using this formula in supposing  $\alpha = 1$ ,  $\varepsilon_a = \varepsilon_{\text{dis, ion}}$  have demonstrated the good consent of calculation data with the experiment [26-28].

The middle densities of the undisturbed flow are favorable for the development of AR as the flow is frozen under low densities ( low numbers  $M$  ) and is equilibrium under high densities ( high numbers  $M$  ) and therefore conditions of a rise of this phenomenon are absent in both cases. And so neutral curves must be closed. But up to now the top density or pressure boundary of AR is not detected. The lower AR boundary is fixed distinctly by experiments in freons and Xe [23,26-28] ( see also Fig.7 of this report).

The Z-form of the percussive adiabat is necessary to arise the phenomenon AR since in this case the dependence  $p = p(v)$  is nonsingle-valued. And so in Ref.[22] the gasdynamic criterion of the shock waves instability was obtained from the percussive adiabat relation. Like the D'jakov criterion this one is limited and is not disclosing the physical reasons of the shock wave instability. In Ref.[26] the series of the better criteria of the instability was obtained. These criteria can be effectively used if the suitable kinetics is available.

The simplest kinetic scheme taking into account the fundamental features of the phenomenon AR ( the considerable rise of concentrations of excited particles, the formation of superequilibrium number of highly excited particles with sufficient life time, collisions of these particles with each other, resulting in the dissociation of one of the particles with complete disactivation ) includes the following reactions [22,28]:



Here  $A_2$  is a two atomic molecule,  $A_2^x$ ,  $A_2^*$  are excited and strongly excited molecules,  $2 \varepsilon(A_2^*) > \varepsilon_d$ ,  $\Delta E$  is the energy releasing during the dissociative disactivation. This kinetic scheme adequately reflecting basic stages of the process AR is simplifying too the real processes.

The analysis of experimental data and of feasible schemes of kinetic processes behind shock waves permitted to elaborate the mechanism of the ionization anomalous relaxation in inert gases. This mechanism gives satisfactory explanation to the nonmonotony of a distribution of the gasdynamic parameters along the relaxation zone observed in experiments. The mechanism includes reactions of the accumulation of the energy of the shock wave in metastable particles, reactions of the transformation of the excitation energy into a form suitable for rapid T-deactivation (the transformation of the excitation energy in the heat), reactions of intensive T-deactivation with regeneration of the metastable particles, processes of emission in lines, processes of the ordinary ionization relaxation. The scheme of the mechanism of the ionization relaxation behind shock waves in the inert gas offered in Ref.[29] is shown in Fig.8. Results of the calculation of the proposed system of equations carried out in the some Ref.[29] are represented in Fig.9,10. The computation showed the presence behind shock waves in Ar of superequilibrium concentrations of components  $A_2^+$ ,  $A_2^{*+}$ ,  $A^+$ , where  $A \equiv Xe$ , and the nonmonotony of a change of gasdynamic parameters along the relaxation zone. Besides, it was ascertained that the formation of superequilibrium concentrations particles  $A_2^+$ , which are able to accumulate the inner energy, coming from other regions by means of the emission, and then to transform it in the heat is necessary for rising anomalies in the gasdynamic structure of the flow behind shock waves. In Ref. [30] the authors carried out the fuller calculation of the flow behind the shock wave front in Xe and computed adiabats at the different distance from the shock front. They discovered that adiabats have Z-form under  $V > 2.5$  km/s and it points to the flow instability (see Fig. 11).

Simultaneously with a development of theoretical researches the detailed experimental investigations of different aspects of AR began. The peculiarities of this phenomenon in molecular gases were studied in free flight [21,23,28,31-34]. These investigations were conducted in gases containing halogens because the shock wave instability in such gases is observed by small numbers  $M$  ( $M \sim 3$ ) while the one in air,  $CO_2$ ,  $CH_4$ ,  $C_2H_2$  is absent up to number  $M \sim 9$  (according to the data of our free flight experiments). As a result of this study it was detected that the location of boundaries of fields of the existence of the instability (the neutral curves  $p_c = p_c(M)$ ) changes with the kind of gas, the concentration of admixture of other gas, the bluntness and dimensions of a body [21,32,33]. It follows from data of graphs of Fig. 12-15. It is seen that neutral curves are displaced in the region of the high pressure and large numbers  $M$  with the decrease of the diameter and the bluntness of a body. In that direction neutral curves are removed with increasing the energy of the gas dissociation. The admixture of gas

having the higher energy of the dissociation to the basic one calls the displacement of neutral curves in the direction of the increase of the number  $M$ .

The intensive instability of the shock wave was discovered in shock tube experiments carried out in Ar, Kr, Xe,  $N_2$ ,  $O_2$ ,  $CO_2$  and other gases [13,15,16,23-28]. These experiments were conducted by the pressure 1-25 Torr, in some tests the pressure was 50 or 100 Torr. A few of experiments and the limited range of the pressure have not allowed to obtain experimental neutral curves in these gases. Neutral curves of inert gases were obtained analytically with using experimental data [26]. Shock tubes investigations were ascertained that the front bifurcation, the weak undulation of the shock wave, the disturbance of the relaxation zone, the nonmonotonic change of gasdynamic parameters behind the shock wave are precursors of large perturbations and destruction of its front [26-28]. In inert gases it was found series of peculiarities of emission: a narrow (less than 1 mm) zone of intense glow immediately behind the shock wave front (Ar,  $M=26$ ,  $p=3$  Torr), a random emission field in  $0.5Ar + 0.5Xe$  mixture and so on [24-28]. These peculiarities (in particular, Ar I and Xe II lines detected in the spectrum of the near zone of the shock wave in Ar and Xe, which are associated with dissociative recombination of  $Ar_2^+$  and  $Xe_2^{++}$ ; the spectrum is obtained both in the shock tube and in the low-density wind tunnel, Fig.16,17) represent unique elementary processes inherent to anomalous relaxation. The investigation of emission spectra in Ar and Xe has demonstrated the leading part of metastable particles in development of AR [26-28].

In the low-pressure tunnel experiments in which an Ar plasma having a metastable particle composition simulating the state behind the shock wave detached from a model at  $M=23$ ,  $p = 0.5$  Torr, an appreciable increase of the heat flux was observed when the concentration of the metastables was increased from 3 to 10 % [26-28] (see also Fig.18).

In free flight experiments it was studied the dependence of the amplitude of shock wave perturbances on number  $M$  at the regimes of AR in different gases and mixture [33,34]. It was revealed that the amplitude value increases with number  $M$  from 0 before the neutral curve to its maximum behind it and then decreases to 0 when the flow becomes equilibrium one. There are no perturbances of shock waves in equilibrium and frozen flows. Decreasing the energy of the dissociation leads to the decrease of the amplitude of shock wave perturbances [33,34] (see Fig.19).

The shock wave perturbation, the turbulization of the inviscid wake are to provoke a rise of the drag of a body flying at regimes of AR. Such increase of the sphere drag (up to 4%) in freon-12 was detected in Refs.[23,26-28] (Fig.20). The inviscid flow turbulization arises because of the local spontaneous heat release in relaxation zone and perturbances of the shock wave which cause the appearance of turbulent vortices of contact surfaces. And so the remote wake at AR regimes looks as a fir-tree [31] (Fig.21).

Thus nonequilibrium physico-chemical processes behind intensive shock waves cause gasdynamic anomalies arising in relaxing media. Since plasma is one of these media, one can expect that similar phenomena exist in plasma while

moving bodies and shock waves in it. This idea has stimulated the investigation of flows arising by the movement of bodies and shock waves in low temperature discharge plasma. The results of these investigations are discussed in the next section of the report.

### 3. Peculiarities of Flow around Bodies and Shock Waves Propagation in Plasma

In this section of the report it is discussed the results of theoretical and experimental investigations of the flow around bodies and of the shock waves propagation in low temperature discharge plasma. These investigations are the logical continuation and the development of our researches of anomalous phenomena arising by the movement of bodies and shock waves in relaxing gases. As a result of these investigations it was revealed series of new and unexpected phenomena including the phenomenon of the anomalous flow around bodies in plasma.

The first photographs of the free flight sphere flowed in the discharge plasma were obtained by Ju.Serov and I.Javor in Ioffe Physico-Technical Institute. These photographs demonstrated the considerable increase of the shock wave detachment from a sphere flying in plasma ( see Fig.22,23 ). Some of them impressed that there was the blasted release of the energy in the shock layer of the sphere. And so the first model of the anomalous flow around bodies in plasma [35] was based on the idea that behind the shock wave in plasma as well as at the regimes of AR in gases the energy of inner degrees of freedom ( in particular, the oscillation energy [36] ) transforms in the heat one. According to the hypothesis the fast energy transformation causes the shock wave acceleration and the change of gasdynamic parameters behind it. But in Ref.[37] it was revealed by the calculation methods that the acceleration of shock waves in plasma is conditioned practically completely by the heat effects. One can make the same conclusion if he will analyze in common all the data of experiments on the velocity of the shock waves propagation in plasma and heat gases [37-43]. This is a reason why we rejected this hypothesis.

The following experimental investigations in shock tubes revealed series of peculiarities of the shock wave propagation in plasma, in particular the shock waves structure change [38-45]. According to Refs.[39,40,45 ] shock waves in plasma have a three-wave structure and consist of leaders, precursors and residual waves ( see Fig.24 ). Velocities of the propagation of the leader  $V_L$ , the precursor  $V_p$  and the residual wave  $V_o$  answer the inequality  $V_L > V_p > V_o$ . So far as the leader is of no noticeable importance in gasdynamic processes, we shall not examine it later on.

The shock wave splitting in plasma and the change of the detachment of the shock wave from a body and of the drag coefficient discovered in free flight experiments testify to the existence of two velocities of the sound frozen or plasmic  $a_p$  and equilibrium or adiabatic  $a_T$ . These velocities satisfy the inequality  $a_p > a_T$ . The value of the adiabatic sound velocity is calculated by usual methods. The value of the plasmic sound velocity was determined from the displacement of

dependencies  $\Delta = \Delta(V)$  ( $\Delta$  is the detachment of the shock wave from a body) or dependencies  $C_x = C_x(V)$  in plasma and in air [46-49]. According to data of measurements of the detachment of the bow shock wave from the sphere [46,47] (Fig.23) and of the drag coefficient of the sphere [48,49] (Fig.25) in air plasma the value of  $a_p$  is  $\sim 1.5 a_T$ . It is necessary to note that the coefficient by  $a_T$  can change with the degree of the excitation of molecules and atoms in plasma. The character of changing the detachment of the shock wave from the sphere and the structure of the shock wave in decaying plasma with time  $t$  points out it [50,51]. According to data of these references the detachment and the structure of shock waves in decaying plasma do not change by  $t \leq 2\text{ms}$  and turn out near ones in undisturbed air by  $t > 200\text{ms}$  (the data of Fig. 26 demonstrate the character of changing the shock wave structure in decaying plasma of air and Ar). It means that the electronic temperature  $T_e$  does not exert the noticeable influence on the sound velocity in plasma  $a_p$  on reaching some threshold of the molecules excitation. And so the estimations of the value of this velocity carried out with using the data of experiments of Ref.[46] ( $T_e = 1-2 \text{ eV}$ ) and of Ref.[48] ( $T_e = 5-6 \text{ eV}$ ) proved identical. Therefore one can take that in case of discharge plasma with  $T_e > 1 \text{ eV}$  the sound velocity is  $a_p \sim 30\sqrt{T}$ . Hence supposing  $\gamma = c_p / c_v = 1.25$  and using usual relations of the normal shock and of the shock wave reflected from the flat wall it is no troubles to calculate the values of the static and stagnation pressure behind the precursor and the pressure behind the precursor reflected from the flat wall. The results of these calculations conducted in Ref.[49] are represented in Fig.27 where it is shown the dependences  $P_{2p} / P_{2b} = f(M_b)$ ,  $P'_{0p} / P'_{0b} = f(M_b)$ ,  $P_{3p} / P_{3b} = f(M_b)$ . Here  $P_2$  is the static pressure behind the shock,  $P'_0$  is the stagnation pressure behind the shock,  $P_3$  is the pressure behind the shock wave reflected from the wall, the indices  $b$  and  $p$  are concerned parameters of the shock wave in cold air and of the precursor in plasma. It is seen on this figure that the static and stagnation pressure behind the shock wave in plasma makes up 40-50 % of the corresponding pressure in cold air. The data of experiments obtained in shock tubes [38,39,41] are confirming this result. The analogous decrease of the stagnation pressure in the air flow (40-60 %) and the increase of the detachment of the shock wave from a body by switching on the glow discharge was registered too in experiments carried out in the aerodynamic tunnel [52].

As it was mentioned above, the shock wave by entering the discharge field is splitted into two (excluding the leader) following each other waves, one of which is high frequency (the precursor) and another is low frequency (the residual wave). The splitting of the shock wave is the specific feature of its propagation in plasma. The amplitude of both waves is considerably less than one in cold air undisturbed by the discharge (see Fig.26). At that time the summary shock wave impulse influencing on the piezoelectric probe remains without any change irrespective of the shock wave propagates in air or in plasma. And so the duration of the impulse in plasma is considerably greater than in air (Fig.26).

According to Refs.[51,53] the precursor and the residual wave in air plasma exist apart during 50 ms after the discharge current interruption ( in these experiments the velocity of the shock wave in cold air was 625 m/s ). The data of Fig.28 give the notion of the character of a change of the ratio of the amplitude of the precursor in Ar and air plasma to the amplitude of the shock wave in cold gases with the time. It is seen on the figure that the relative value of the precursor amplitude changes in air plasma from 0.24 (  $\tau = 0$  ) to 0.42 (  $\tau = 50\text{ms}$  ). The precursor amplitude in plasma is less than the residual wave amplitude. The values of amplitudes are evened in 6-7ms after the interruption of the discharge current. The complete restoration of the amplitude and the structure of shock wave in decaying plasma to the same in undisturbed cold air finishes in 100-120s. There are the similar effects in decaying argon plasma. But in this case the apart existence of the precursor and the residual wave is observed by  $\tau < 150\text{ms}$  and in 15 ms after the current interruption the precursor and residual wave amplitudes prove to be equal. The residual wave in plasma of air and Ar erodes a great deal and resembles few the real shock wave and so it is not seen at the photographs obtained in free flight experiments. It means that the Pitot loss in the residual wave is not so much as in the precursor and by virtue of that fact the values of the drag and other aerodynamic coefficients of bodies moving in plasma with the supersonic velocity are appointed in the main by the precursor. As the precursor is formed by the acoustic waves of the high frequency, the parameter of modeling flows can be the Mach number  $M = V / a_p$ , where  $a_p$  is the frozen velocity of the sound ( in air plasma  $a_p \approx 30 \sqrt{T}$  ).

Taking it into account and knowing that the drag coefficient ratio  $\bar{C}_x = C_x \cdot \rho V^2 / 2P_0'$  is not depending on the ratio of specific heats [54] (see Fig.29), we (following Ref.[49]) shall present the results of measuring the drag coefficient of the sphere in plasma [48] in the form of the graphic dependence  $\bar{C}_x = \bar{C}_x (M)$  ( Fig.30). The values of the coefficient  $\bar{C}_x$  of sphere in plasma and as well in other media are plotted on the diagram. Looking at the diagram one can conclude that the values  $\bar{C}_x$  of the sphere in plasma and in other media are near with each other. If one supposes that this effect takes place in case of other bodies too (like the data of Fig.29 ), it gives an opportunity of evaluating the drag coefficient of any body in plasma with using the data of measurement of this coefficient in any gas ( in air for example ). The method of evaluating is evident:

$$C_{xp} = C_{xs} \cdot \bar{P}_{op}' / \bar{P}_{os}', \quad (4)$$

where indices p and s concern accordingly plasma and gas.

As the drag of a body flying with the set velocity is directly proportional to  $\rho C_x$ , one can influence on its value not only by the  $C_x$  change but by the change of the density which depends on both the gas temperature and the degree its dissociation. So the summary drag in plasma by conditions [48] decreases 4-10 times as the value of the drag in cold air.

In Refs.[26,50,55] it is studied the character of the change of the heat flux in plasma but the data obtained was discrepant. So the results of Ref.[26] demonstrate the increase of the heat flux with the concentration of metastables in Ar plasma (see Fig.18). The analogous increasing of the heat flux was fixed in air plasma [55]. At that time in Ref.[50] it was compared the results of measurements of the ablation of the sphere flying with the velocity  $V = 2310$  m/s in plasma and air heated to the plasma temperature ( $T = 1400$  K) and it was discovered the substantial decrease of its value in decaying plasma ( $\tau = 1.7$ ms)  $\sim 4$  times as in air that points at decreasing the heat flux in plasma. The decrease of the ablation and the heat flux in plasma in comparison with air can be connected with decreasing number  $M$  in plasma and the stagnation temperature behind the shock wave.

Thus the whole complex of data obtained in free flight, in shock tubes and in aerodynamic tunnels points that the reason of gasdynamic anomalies arising by the movement of shock waves and bodies in plasma is peculiarities of the propagation of the sound in it. These peculiarities are caused by the difference of parameters of relaxation processes (time and velocities of relaxation and etc.) under the propagation of small perturbances in air or other relaxing gases and in plasma. Therefore the investigation of physico-chemical processes by the propagation of sound and shock waves in plasma is of the greatest interest nowadays. But similar investigations were carried out not much till now and they have a contradictory character.

Some experimental investigations of the behavior of the charged component of discharge plasma by passing it the shock wave were carried out in shock tubes of the electrical discharge type [56-58]. The experiments were conducted in the longitudinal discharge under conditions of the restriction of the plasma field by walls of the working sections of shock tubes. In Ref.[59] the vertical discharge did not touch shock tube walls. Shock waves in all the articles were generated by impulse electrical discharger. In some shock tubes one could obtain usual shock waves with the long uniform profile of the pressure behind their fronts and shock waves of a blast type. Single and double probes, SHF- interferometers, mass-spectrometers, schlieren-systems and other devices were used in these experiments for the measurement of plasma parameters.

As a result of investigations in Refs.[56,57] it was revealed that there is the jumping increase of the electron concentration  $n_e$  at the shock front in argon and nitrogen plasma (see Fig.31,32) with  $n_e$  increasing by the discharge current growth. This phenomenon is accompanied by the jumping decreasing of the electron temperature  $T_e$  behind the shock front 1.5-2 times as before it (Fig.31,32). The value of the  $n_e$  jump at the front of the shock wave depends on the orientation of the electric fields of the discharge and of the shock wave (the ambipolar field of the shock wave appears because of the diffusion of electrons at its front). The value of the  $n_e$  jump behind the shock front by the identical orientation of the electric fields is considerably larger than by the usual gasdynamic compression. The electron concentration under the opposite orientation of the fields remains the same as in

case of the gasdynamic compression. There are the similar uneven changes of the concentrations of ions  $N_2^+$ ,  $N^+$ ,  $O^+$ ,  $OH^+$ ,  $H_2O^+$ ,  $N_3^+$  at the shock wave front in nitrogen discharge plasma ( see Fig.33). It is necessary note that changes of the concentration of charged particles and of the electron temperature correspond with the character of the change of the density behind the shock wave.

In Ref.[58] it was confronted data of measurements of the pressure  $p$ , the density  $\rho$ , the luminosity of plasma  $J$  and the electron concentration  $n_e$  while passing the shock wave through plasma of a glow discharge ( see Fig.34 ). It was ascertained that in plasma the shock wave erodes, the jump  $n_e$  arises at its front and the plasma luminosity decreases. All the effects correlate with each other and with the character of the change of the density at the shock wave front. So the maximum  $n_e$  conforms the minimum of the luminosity of plasma that points at the existence of processes of the stimulated ionization with the participation of the excited particles at the shock front in plasma.

Conducting the experiments in the decaying plasma of  $CO_2$  the authors of Ref.[58] discovered two maxima  $n_e$  ( Fig.35 ). The former was identified with the leader-precursor. The velocity of its propagation (  $\sim 50\text{km/s}$  ) is much more than the shock wave velocity. The second of the maxima is caused by the compression of the electron component of plasma.

In Refs.[59,60] it was fulfilled the probe measuring in the free glow discharge in air. The measurements were conducted in the steady-state discharge and in the discharge perturbed by moving shock waves. It was obtained the radial  $T_e$  distribution in the steady-state discharge and was revealed that  $T_e$  is constant and is equal 1-2 eV practically in all the discharge field. The concentration  $n^+$  has the bell form with the maximum at the discharge axis ( $n^+ \sim 8 \cdot 10^{11}$ , see Fig. 36 ).

The double probe investigation of the plasma conductivity [59] allows to ascertain that shock waves influence on the concentration  $n^+$ . The  $n^+$  dependence on the time is not monotonous and reflects the three-wave structure of shock waves in plasma. The concentration  $n^+$  decreases by moving the leader, the precursor and the residual wave in plasma. The first minimum  $n^+$  is placed behind the precursor front with the value of the minimum depending on the probe location. The  $n^+$  concentration is minimum at the discharge axis. At the same time the single probe investigation of the plasma does not display the jump potential in plasma while passing shock waves.

The experimental discovering of the compound structure of shock waves in plasma stimulated theoretical researches of the distribution of plasma parameters near the front of shock waves moving in weakly ionized gas ( see e.g. Refs.[61,62]). Although these researches did not ascertain the nature of the anomalous phenomena nevertheless they confirmed the existence of electrical precursors before shock waves moving in plasma.

Studying the time of the existence of the anomalous dynamic properties of decaying plasma it is possible to clean up the character of physico-chemical processes taking place under the propagation of shock waves in low temperature



plasma. First such investigations were carried out in Ref.[63], their results are shown in Fig.38 where it is demonstrated the dependencies of the propagation velocity and the amplitude of the shock wave moving in decaying plasma on the time after interrupting the current of the discharge. In this reference it was revealed that in the diapason of the time  $0 < \tau < \tau_1 = 1\text{ms}$  the shock wave velocity is practically invariable and then it decreases exponentially ( the constant of the time  $\sim 10\text{ms}$  ) approaching the velocity of the shock wave in cold air in the time  $\sim 100\text{s}$ . The amplitude of the shock wave under  $\tau < \tau_1 = 1\text{ms}$  after interrupting the discharge remains without changes (  $A_p / A_0 \sim 0.2$  ) too and then it increases monotonously up to the value  $A_0$  (  $A_p$ ,  $A_0$  are amplitudes of shock waves in plasma and in cold air ). The intensity of the luminescence of plasma decreases sharply after the interruption of the discharge current (the time constant  $\tau \sim 1.5\text{mks}$  ) and then decreases slowly with the time constant  $\tau \sim 3.5\text{ms}$ . Though the times of these processes correlate each other, nevertheless in this reference these times were not compared to the characteristic times of the relaxation processes in plasma.

In detail the influence of the shock wave on the piezoprobe locating in the decaying plasma was studied in Refs.[51,53]. The specific peculiarity of the shock wave propagation in plasma is its splitting by entering the discharge field into two following each other waves: the precursor ( the high frequency part of the shock wave ) and the residual wave ( the low frequency part of the shock wave ). In these Refs.[51,53] it was studied the dependence of the signal of the piezoprobe registering both waves on the time. The experiments were carried out in decaying plasma of the glow discharge under the pressure  $p = 33\text{ Torr}$  and the shock wave velocity ( in the absence of discharge )  $V = 625\text{m/s}$ . As a result of these researches supplemented with Ref.[63] it was ascertained the next characteristic times of the process of the propagation of the shock wave in decaying plasma:  $\tau_2 = 6-7\text{ms}$  is the time of evening the amplitudes of the precursor and the residual wave;  $\tau_3 \sim 50\text{ms}$  is the time of separate existence of the precursor and the residual wave;  $\tau_4 \sim 100\text{s}$  is the time of restoration of the amplitude and the structure of the shock wave in decaying plasma to the values in cold air.

In Ar it was ascertained only two of the characteristic times :  $\tau_2 \sim 15\text{ms}$  is the time of equalizing the amplitudes of the precursor and the residual wave;  $\tau_3 \sim 150\text{ms}$  is the time of separate existence of the precursor and of the residual wave.

The estimates conducted in Ref.[53] show that the time of decreasing the concentration of the charged particles in decaying plasma one hundred times is equal  $\sim 2\text{ms}$ . This time correlates with the time  $\tau_1$ . During the time  $\tau_1$  the amplitude of the shock wave and its velocity are not changing. The rest of the characteristic times (excluding  $\tau_4$ ) was not identified.

The investigation of the shock wave reflected by the plane wall was carried out in Refs.[64,65]. The experiments were conducted by the pressure  $p = 3-30\text{ Torr}$ , the current density in the discharge  $j = 30\text{mA/cm}^2$ , the velocity of the shock wave

in cold air  $V_0 = 400-600 \text{ m/s}$ , the duration of the flow of shock-compressed gas  $t = 150-200 \text{ mks}$ . The fall shock wave in plasma was of the typical three-wave structure ( the leader, the precursor, the residual wave ). Under the reflection of the shock wave propagating in plasma from the wall there is the interaction of its falling and reflected elements. That conducts to much more erosion of the reflected shock wave than the falling wave ( see Fig.39 ). At the same time the specific plasma formation arises near the plane wall. All first it envelopes the field  $\sim 3.5 \text{ cm}$  from the wall, then it squeezes into the region  $\sim 2 \text{ cm}$  from the wall. The time of its arising is  $\sim 200 \text{ ms}$ , if the experimental conditions are following :  $V_0 = 500 \text{ m/s}$ ,  $p_0 = 12 \text{ Torr}$ ,  $\rho_e / \rho_0 = 1$ , where index  $e$  is concerned the plasma formation, index  $0$  is concerned cold air. This formation is founded in the frozen state for a sufficiently long time. Its life time depends on the pressure :  $\tau = 500 \text{ ms}$  under  $p_0 = 12 \text{ Torr}$  and  $\tau = 2000 \text{ ms}$  under  $p_0 = 30 \text{ Torr}$ . After that the disintegration of the plasmic formation takes place. The concentration of the electrons by all that decreases the first as  $\sim 1.5$  times and then restores up to its initial level existed before the disintegration of this formation [65]. And so the plasma conduction decreases as  $\sim 2$  times. Thus the plasma near walls shows the higher dielectrical properties than usual plasma of the glow discharge .

Of course the obtaining of the new information on details of physico-chemical processes proceeding by the movement of shock waves in plasma is an important result of the researches carried out , but the role of these processes in the rise of the anomalies of the propagation of sound and shock waves in non-equilibrium plasma is not disclosed up to date.

Reviewing all the set forth information we can affirm that all the gasdynamic anomalies arising by the movement of shock waves and bodies in non-equilibrium plasma are stipulated by the peculiarities of the propagation of sound waves in relaxing media and in the end by the physico-chemical processes taking place in plasma.

*Bacapa*  
05.01.98

*Bedu*  
05.01.98

## REFERENCES

1. Дунаев Ю.А., Мишин Г.И. Баллистическая труба для измерения коэффициентов сопротивления в свободном полете. Изв.АН СССР, Механика и машиностроение, № 2, 1959, с.188-190.
2. Бедин А.П. Баллистическая установка БУ-88 ФТИ РАН ( конструкция, методы и результаты исследований аэродинамических характеристик тел ). Препринт ФТИ РАН, № 1680, СПб., 1996, 40 с.
3. Басаргин И.В., Менде Н.П., Мишин Г.И. и др. Гиперзвуковая баллистическая установка. В кн.: Физико-газодинамические баллистические исследования, Л.,Наука,1980, с.171-179.
4. Басаргин И.В., Мишин Г.И., Федотов А.А. Автоматизированная установка для исследования динамических свойств ударных волн в газоразрядной плазме. Препринт ФТИ РАН № 1642, СПб., 1995, 44с.
5. Борисов В.Н., Мишин Г.И. Искровой источник света для газодинамических исследований. ЖНПФК, 1973, №1, с.22-25.
6. Златин Н.А., Красильщиков А.П., Мишин Г.И. и др. Баллистические установки и их применение в экспериментальных исследованиях. М., Наука, 1974, 344 с.
7. Борисов В.Н., Дементьев И.М., Ковалев П.И. и др. Импульсные источники света для баллистических исследований. В кн.: Физико-газодинамические баллистические исследования. Л., Наука, 1980, с.193-199.
8. Мишин Г.И., Родичева И.Н. Автоматическая синхронизирующая аппаратура для баллистических исследований. В кн.: Аэрофизические исследования сверхзвуковых течений, М.-Л., Наука, 1967, с.184-187.
9. Бедин А.П., Мишин Г.И., Чистякова М.В. Исследование аэродинамических характеристик тел затупленной формы в воздухе. В кн: Физико-газодинамические баллистические исследования, Л., Наука, 1980, с.9-24.
10. Бедин А.П. Исследование нестационарных аэродинамических характеристик затупленных тел малого удлинения в свободном полете. В кн.: Физико-газодинамические баллистические исследования, Л., Наука, 1980, с.48-56.
11. Бедин А.П., Троицкий М.Н. Юстировка оптических систем баллистической установки. Препринт ФТИ АН СССР № 1462, Л.,1990, 19с.
12. Hilton W.F. High-Speed Aerodynamics , London, 1952, 598p.
13. Griffiths R.W., Sandeman R.J., Hornung H.G. The Stability of Shock Waves in Ionizing and Dissociating Gases.- J.Phys.D.: Appl. Phys.,1976, v.9, No.12, p.1681-1691.
14. Дьяков С.П. Об устойчивости ударных волн.-ЖЭТФ,1954, т.27, в.3(9), с.288-295.

15. Glass I.I., Liu W.S. Effects of Hydrogen Impurities on Shock Structure and Stability in Ionizing Monatomic Gases. Part I, Argon-J. Fluid Mech., 1978, v.84, p.55.
16. Гордеев В.Е. Пульсирующая детонация и неустойчивость ударных волн в релаксирующих газах. ДАН, 1978, т.239, с.117-119.
17. Барышников А.С., Бедин А.П., Масленников В.Г. и др. О неустойчивости фронта головной ударной волны. Письма в ЖТФ, т.5, 1979, с.281-284.
18. Барышников А.С., Бедин А.П., Мишин Г.И. и др. Релаксационная неустойчивость ударных волн. В кн: Физико-газодинамические баллистические исследования. Л., Наука, 1980, с.34-42.
19. Барышников А.С., Бедин А.П., Мишин Г.И. и др. Релаксационная неустойчивость ударных волн в газах. Доклад на 5 Всесоюзном съезде по ТПИМ, Алма-ата, 1981.
20. Барышников А.С., Бедин А.П., Деревянко В.Г. и др. Статистические характеристики флуктуаций течения и механизмы неустойчивости ударной волны в релаксирующем газе. Препринт ФТИ, № 816, Л., 1983, 33 с.
21. Бедин А.П., Климов А.И., Коблов А.Н. и др. Исследование релаксационной неустойчивости ударных волн в молекулярных газах при свободном полете тел. Материалы Международной школы - семинара "Высокотемпературная газодинамика, ударные трубы и ударные волны", Минск, 1983.
22. Барышников А.С., Скворцов Г.Е. Неустойчивость ударных волн в релаксирующей среде. ЖТФ, т.49, в.11, 1979, с.2483-2485.
23. Бедин А.П., Мишин Г.И., Скворцов Г.Е. Аномальная релаксация при сверхзвуковом течении многоатомных газов. Письма в ЖТФ, т.7, в.10, 1981, с.613-618.
24. Тумакаев Г.К., Масленников В.Г., Серова Е.В. О неустойчивости течения за ударными волнами большой интенсивности в одноатомных газах. Письма в ЖТФ, т.6, в.6, 1980, с.354-358.
25. Рязин А.П. Ионизационная неустойчивость ударной волны в ксеноне. Письма в ЖТФ, т.6, в.9, 1980, с.516-520.
26. Мишин Г.И., Бедин А.П., Ющенко Н.И. и др. Аномальная релаксация и неустойчивость ударных волн в газах. ЖТФ, т.51, в.11, 1981, с.2315-2324.
27. Бедин А.П., Мишин Г.И., Рязин А.П. и др. Аномальная релаксация и неустойчивость ударных волн в газах. Материалы Международной школы-семинара "Высокотемпературная газодинамика, ударные трубы и ударные волны", Минск, 1983.
28. Bedin A.P., Mishin G.I., Ryazin A.P. and oth. Abnormal Relaxation and Instability of Shock Waves in Gases. In: Gas Dynamics, Nova Science Publishers Inc. N.Y., 1992, p.69-80.
29. Ющенко Н.И., Мишин Г.И., Роцин О.В. Механизм аномальной релаксации в ударных волнах инертных газов. Письма в ЖТФ, т.11, в.9, 1985, с.517-524.

30. Григорьев В.Г., Мишин Г.И., Ющенко Н.И. и др. Распределение параметров за фронтом сильной ударной волны в инертных газах и неустойчивость, связанная с аномальной релаксацией. Письма в ЖТФ, т.12, в.4, 1986, с.224-231.
31. Бедин А.П., Мишин Г.И. Об особенностях следа за телами, летящими со сверхзвуковой скоростью в аномально релаксирующих газах. Письма в ЖТФ, т.7, в.11, 1981, с.696-700.
32. Бедин А.П. Эффекты аномальной релаксации в смесях молекулярных и одноатомных газов. Письма в ЖТФ, т.14, в.24, 1988, с.2282-2285.
33. Бедин А.П., Троицкий М.Н. Релаксационная неустойчивость ударных волн при обтекании тел молекулярными газами. Материалы 5 Всесоюзной школы-семинара по современным проблемам механики, Иркутск, 1990.
34. Бедин А.П. Особенности релаксационной неустойчивости ударных волн в молекулярных газах на примере трифториодметана. ЖТФ, т.59, в.8, 1989, с.152-155.
35. Мишин Г.И., Бедин А.П., Явор И.П. Параметры газа за ударной волной при аномальной релаксации. Письма в ЖТФ, т.8, в.3, 1982, с.182-185.
36. Бакшт Ф.Г., Мишин Г.И. Влияние колебательной релаксации на параметры ударных волн в плазме молекулярных газов. ЖТФ, т.53, в.5, 1983, с.854-857.
37. Войнович П.А., Ершов А.П., Пономарева С.Е. и др. Распространение ударных волн в плазме продольного тлеющего разряда в воздухе. ТВТ, т.29, №3, 1991, с.582-590.
38. Басаргин И.В., Мишин Г.И. Предвестник ударной волны в плазме тлеющего разряда. Письма в ЖТФ, т.15, в.8, 1989, с.55-60.
39. Гридин А.Ю., Климов А.И. Структура ударной волны в неравновесной плазме (выделение энергии, запасенной в разрядной плазме за ударной волной). ХФ, т.12, №3, 1993, с.363-365.
40. Гридин А.Ю., Климов А.И., Ходатаев К.В. Исследование распространения ударных волн в неоднородном поперечном импульсном разряде. ТВТ, т.32, № 6, 1994, с.486-490.
41. Басаргин И.В., Мишин Г.И. Газодинамический предвестник ударной волны в плазме тлеющего разряда. В кн.: Основные результаты научной деятельности 1989/90, ФТИ АН СССР, Л.1991, с.100-103.
42. Басаргин И.В., Мишин Г.И. Распространение ударных волн в плазме поперечно и продольно ориентированного тлеющего разряда. Препринт ФТИ АН СССР, № 880, Л., 1984, 22 с.
43. Басаргин И.В., Мишин Г.И. Распространение ударных волн в плазме поперечного тлеющего разряда в аргоне. Письма в ЖТФ, т.11, в.4, 1985, с.209-215.
44. Гридин А.Ю., Климов А.И., Молевич Н.Е. Распространение ударных волн в плазме тлеющего разряда. ЖТФ, т.63, в.3, 1993, с.157-162.

45. Мишин Г.И., Климов А.И., Гридин А.Ю. Измерения давления и плотности в ударных волнах в газоразрядной плазме. Письма в ЖТФ, т.17, в.16, 1991, с.84-89.
46. Мишин Г.И., Серов Ю.Л., Явор И.П. Обтекание сферы при сверхзвуковом движении в газоразрядной плазме. Письма в ЖТФ, т.17, в.11, 1991, с.65-71.
47. Mishin G.I., Serov Yu. L., Yavor I.P. Experimental Investigation of Supersonic Flight of a Sphere in Weakly Ionized Air. In: Proc. of the 2 nd International Conference on Experimental Fluid Mechanics, 1994, Torino, Italy, p.750-754.
48. Бедин А.П., Мишин Г.И. Баллистические исследования аэродинамического сопротивления сферы в ионизованном воздухе. Письма в ЖТФ, т.21, в.1, 1995, с.14-19.
49. Бедин А.П. Об особенностях течений низкотемпературной газоразрядной плазмы. Письма в ЖТФ, т.23, в.16, 1997, с.88-93.
50. Серов Ю.Л., Явор И.П. Абляция при сверхзвуковом движении тела в плазме. ЖТФ, т.65, в.3, 1995, с. 38-45.
51. Басаргин И.В., Мишин Г.И. Эволюция аномальных динамических свойств распадающейся плазмы тлеющего разряда. ЖТФ, т.66, в.7, 1996, с.198-203.
52. Мишин Г.И., Климов А.И., Гридин А.Ю. Продольный электрический разряд в сверхзвуковом потоке газа. Письма в ЖТФ, т.18, в.15, 1992, с.86-92.
53. Барышников А.С., Басаргин И.В., Дубинина Е.В. и др. Перестройка ударной волны в плазме затухающего разряда. Письма в ЖТФ, т.23, в.7, 1997, с.18-22.
54. Бедин А.П., Мелешко В.П., Мишин Г.И. и др. Влияние отношения удельных теплоемкостей среды на аэродинамические характеристики затупленных тел. В кн.: Физико-газодинамические баллистические исследования, Л., Наука, 1980, с.25-33.
55. Грачев Л.П., Грицов Н.Н., Есаков И.И. и др. Нагрев тела в сверхзвуковом потоке плазмы. ЖТФ, т.65, в.1, 1995, с. 167-171.
56. Чутов Ю.И. Экспериментальное исследование ударных волн в частично ионизованной газоразрядной плазме. П МТФ, №1, 1970, с.124-130.
57. Чутов Ю.И., Подольский В.Н. Ударные волны в газоразрядной плазме. Инженерно-физический журнал, т.62, № 5, 1992, с.707-713.
58. Горшков В.А., Климов А.И., Мишин Г.И. и др. Особенности поведения электронной плотности в слабоионизированной неравновесной плазме при распространении в ней ударной волны. ЖТФ, т.57, в.10, с.1893-1898.
59. Басаргин И.В., Мишин Г.И. Зондовые исследования ударных волн в плазме поперечного тлеющего разряда. Письма в ЖТФ, т.11, в.21, 1985, с.1297-1303.
60. Басаргин И.В., Васильев А.П. Зондовые измерения в свободном тлеющем разряде в воздухе при средних давлениях. Препринт ФТИ РАН, №1643, 1995, 25 с.

- 61.Найдис Г.В. Пространственное распределение параметров плазмы вблизи фронта ударной волны в газовом разряде. ТВТ, т.29, №1, 1991, с.15-20.
- 62.Теселкин С.Ф. Диффузионный предвестник ударной волны в слабоионизованной плазме электроотрицательного газа. Письма в ЖТФ, т.17, в.16, 1991, с.50-55.
- 63.Климов А.И., Коблов А.Н., Мишин Г.И. и др. Распространение ударных волн в распадающейся плазме. Письма в ЖТФ, т.8, в.9, 1982, с.551-554.
- 64.Мишин Г.И., Климов А.И., Гридин А.Ю. Отражение ударных волн от плоской стенки в слабоионизованном воздухе. Письма в ЖТФ, т.18, в.6, 1992, с.37-44.
- 65.Гридин А.Ю., Климов А.И. Самоорганизация энергоемких плазменных структур за отраженной ударной волной в газоразрядной плазме. ХФ, т.12, №3, 1993, с.316-319.
- 66.Merilo M., Morgan E.J. Total Ionization Times in Shock- Heated Noble Gases.- J. Chem. Phys., v.52, N5, 1970, p.2192-2198.
- 67.Простнев А.С., Ющенкова Н.И. Механизм электронной релаксации за фронтом сильных ударных волн. Письма в ЖТФ, т.8, №9, 1982, с.523-527.
- 68.Красильщиков А.П., Подобин В.П. Экспериментальное исследование аэродинамических характеристик шара в свободном полете до чисел  $M \sim 15$ .-Изв. АН СССР, Механика жидкости и газа, 1968, №4, с.190-193.
- 69.Мишин Г.И. Исследование коэффициента сопротивления сферы при сверхзвуковых скоростях в газах с различным отношением удельных теплоемкостей. ЖТФ, т.31, в.4, 1961, с.495-498.
- 70.Мишин Г.И. Зависимость коэффициента сопротивления сферы при сверхзвуковых скоростях от отношения удельных теплоемкостей среды. В кн.: Аэрофизические исследования сверхзвуковых течений. М.-Л., Наука, 1967, с.192-196.
- 71.Krumins M.V. Drag and Stability of Various Mars Entry Configurations.- In:19th Congress of International Astronautical Federation. Rep.N138, N4, 1968.

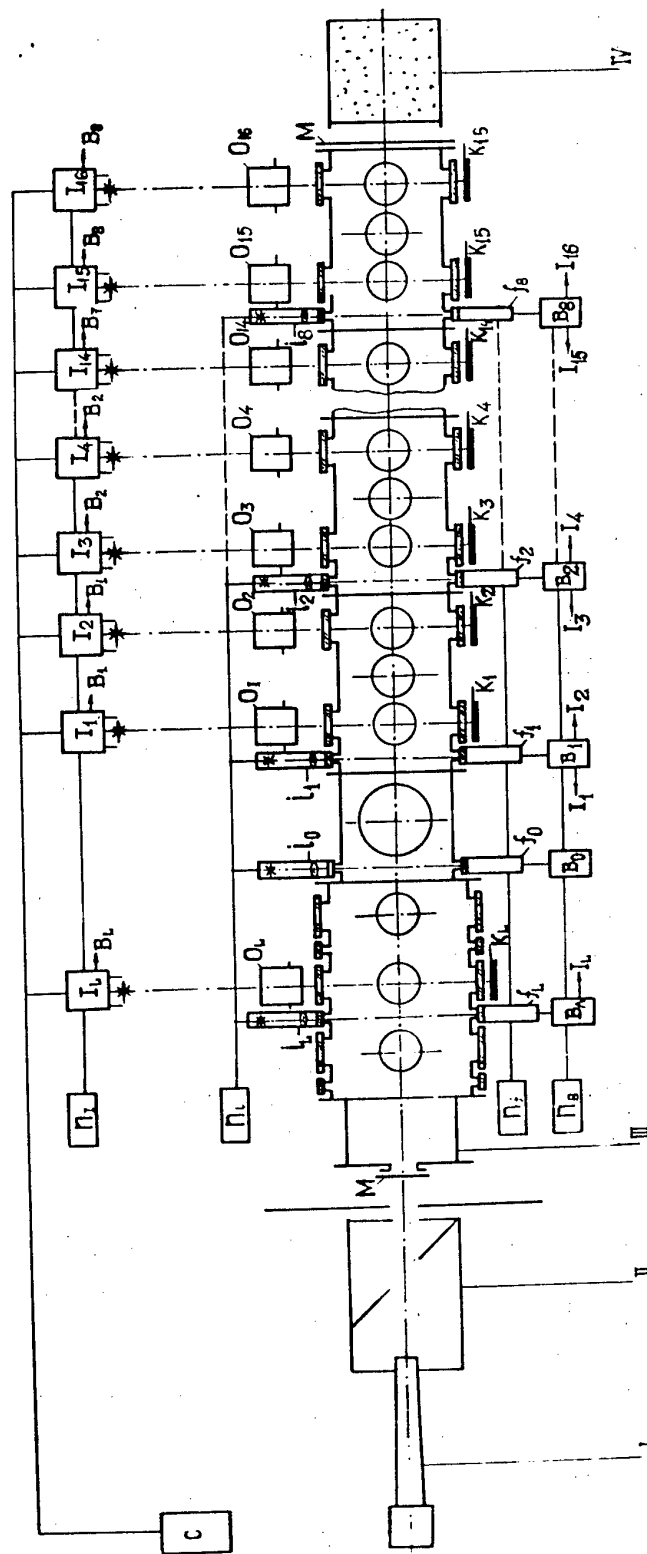


Fig. 1. Scheme of ballistic range BU-88 FTI RAN: I) gun; II) section of model-case separation; III) pressurized chamber; IV) bullet collector; c) chronographs;  $n_n$ ) feeding blocks;  $B_n$ ) synchronization blocks;  $I_n$ ) spark generators;  $O_n$ ) objectives;  $i_n$ ) slit light sources;  $k_n$ ) photomultipliers;  $k_n$ ) photocassettes;  $M$ ) membranes; index L-laser systems.



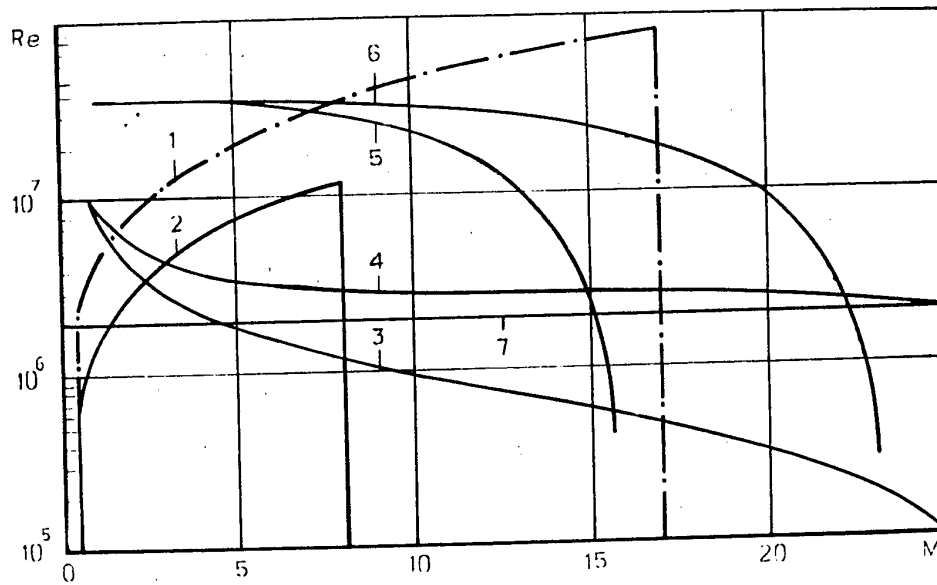


Fig.2 Diapason of change of numbers  $M$  and  $Re$  in free flight experiments: 1)BU-88, freon-12; 2)BU-88, air; 3)trajectory of cosmic probe, enter velocity  $V_e = 8 \text{ km/s}$ ; 4)trajectory of cosmic probe,  $V_e = 11 \text{ km/s}$ ; 5)trajectory of middle-range rocket; 6)trajectory of long-range rocket; 7) $Re = 2 \cdot 10^6$ .

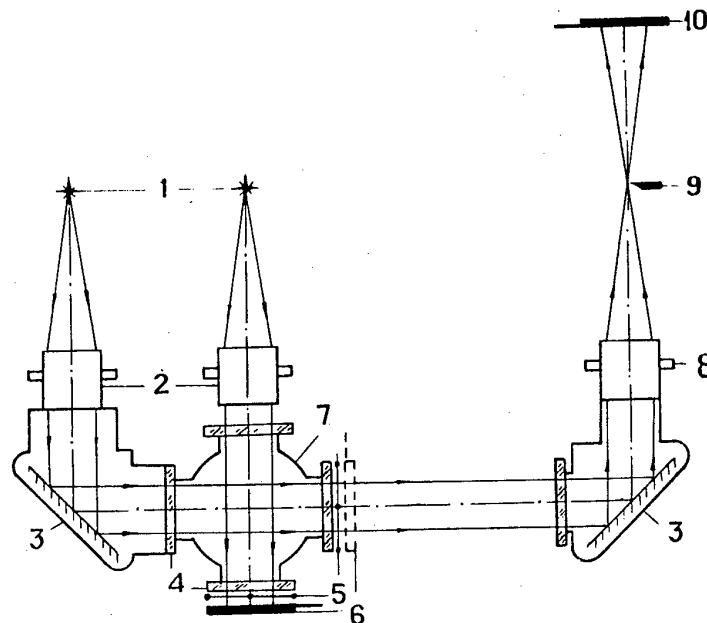


Fig.3. Optical scheme of BU-88 installation: 1) spark sources; 2,8) objectives; 3)turn mirrors; 4) glass window; 5) coordinates system; 6,10) cassette; 7)pressurized chamber; 9) knife.

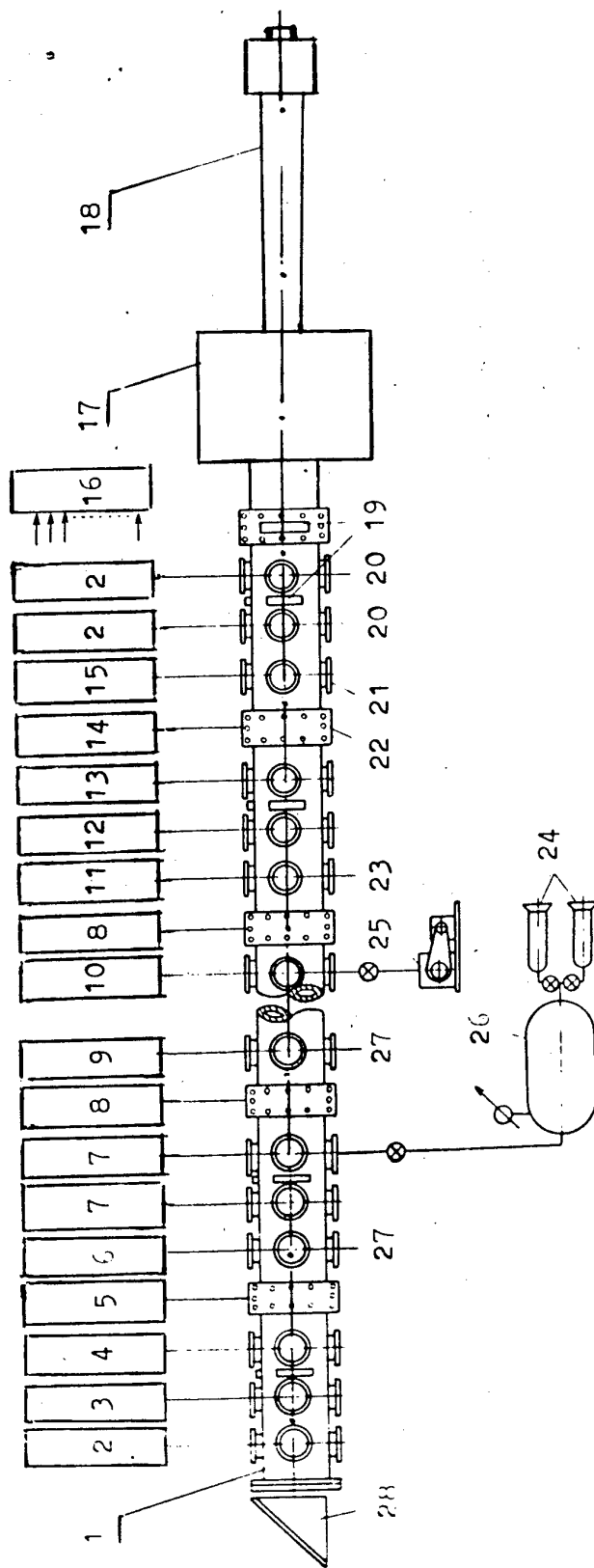


Fig. 4. Scheme of ballistic range GBU: 1) pressurized chamber; 2) schlieren system; 3) five-channel radiometer of the visible spectrum; 4) spectrum recorder MRS-1; 5) one-channel radiometer with the monochromator; 6) schlieren device IAB-451; 7) SHF-probe; 8) double SHF-probe; 9) Mach-Zender interferometer; 10) combined interferometer-spectrometer system; 11) waiting photorecorder; 12) two-channel radiometer; 13) spectrometer; 14) SHF-radiometer; 15) HF-bridge; 16) counter-timers; 17) receiver; 18) gun; 19) slit window; 20) spark generators; 21) viewing window; 22) hatch; 23) pulse lamp; 24) gas-bags; 25) pump; 26) mixer; 27) laser OGM-20; 28) bullet-collector.

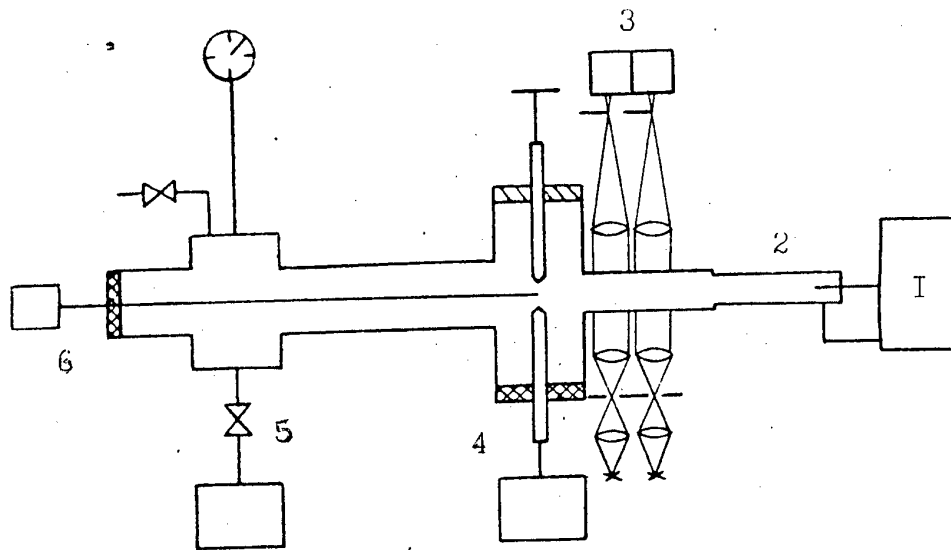


Fig.5. Scheme of electrical discharge shock tube: 1) electrical discharger ; 2) shock tube; 3) two-channel schlieren system; 4) discharger chamber ; 5) pressurized chamber with vacuum equipment ; 6) shifted bar with probes.

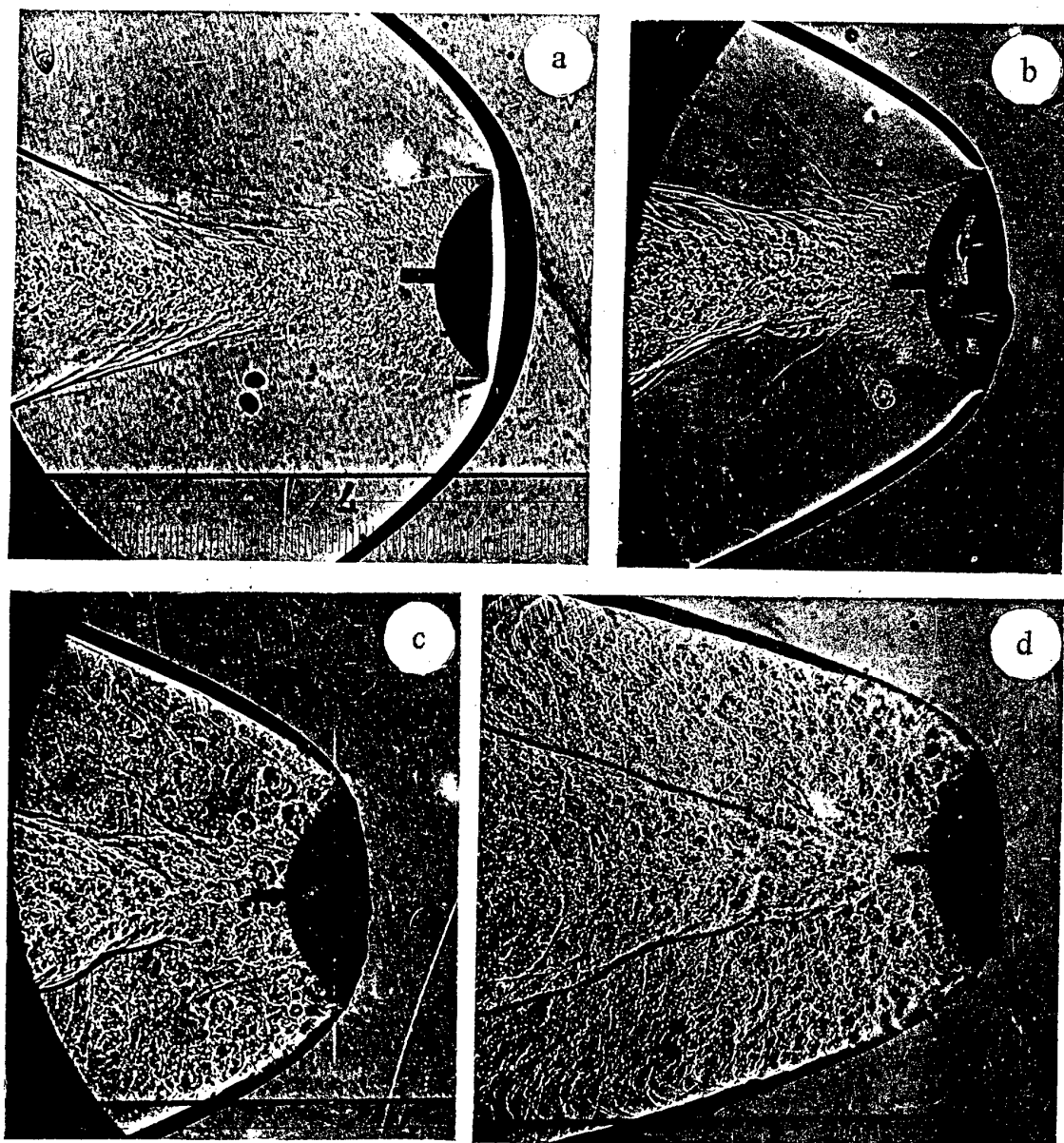


Fig.6. Flow around segmental disk ( $R/d=1.5$ ;  $d=28\text{mm}$ ) in freon-12,  $p=0.04\text{MPa}$ , number  $M$  : a)2.6; b)3.9; c)4.3; d)6.7.

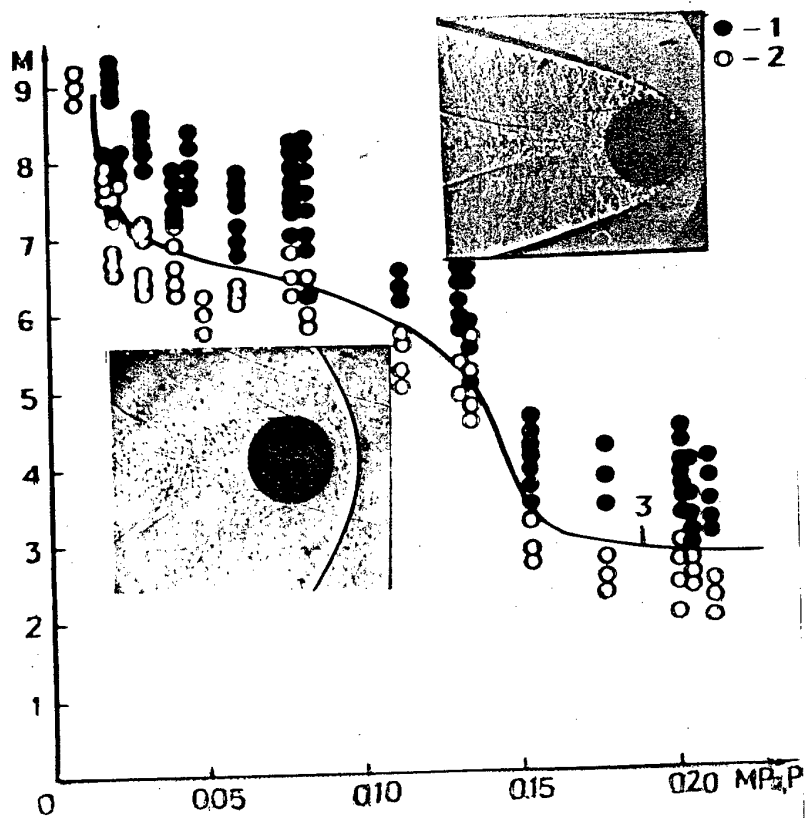


Fig.7. Neutral curve for sphere  $\varnothing 10\text{mm}$  in freon-12: 1) flow is unsteady; 2) flow is steady; 3) neutral curve.

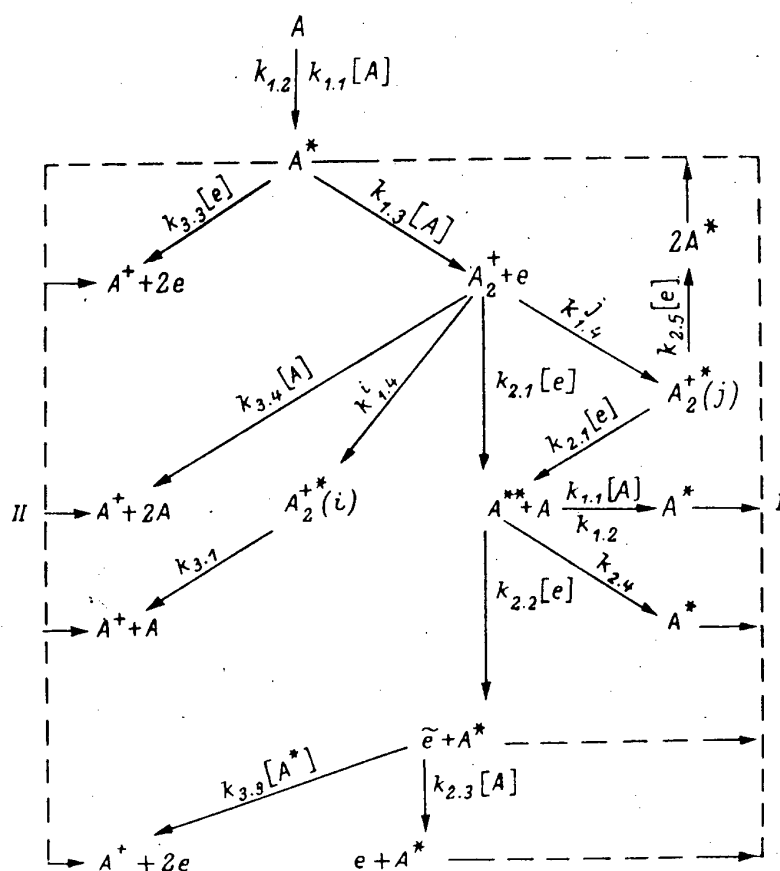


Fig.8. Scheme of mechanism of ionization relaxation behind shock waves in inert gas [29]: I-channel of anomalous relaxation with regeneration of excited particles  $A^*$ ; II-channel of relaxation with irreversible destruction of particles  $A^*$ ,  $A_2^+$ .

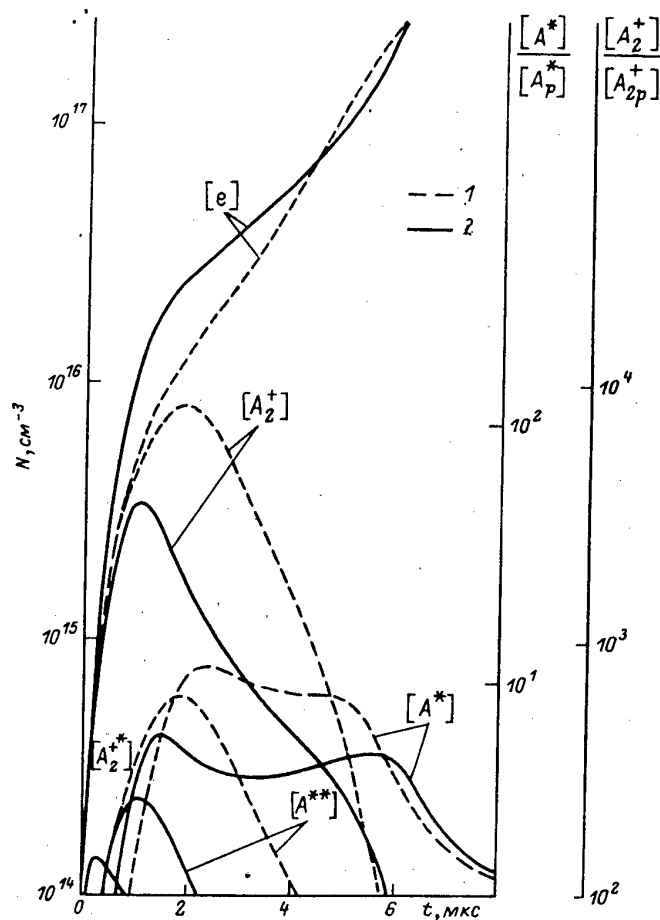


Fig.9. Distribution of components concentration behind shock wave in Xe [29].

$[A] \equiv [Xe]$ . Parameters before shock:  $M_1 = 16.8$ ,  $\rho_1 = 3.3 \cdot 10^{-5} \text{ g/cm}^3$ ,  $T_1 = 300 \text{ K}$ .  $[A^*]_1 = [A^{**}]_1 = 3 \cdot 10^{12} \text{ cm}^{-3}$ ;  $[e]_1 = 10^{13} \text{ cm}^{-3}$ . Kinetic coefficients,  $\text{cm}^3/\text{s}$ :  $k_{1,1} = 2.5 \cdot 10^{-5} \cdot \sqrt{T} \cdot \exp(-104400/T)$ ;  $k_{1,3} = 1.7 \cdot 10^{-8.45} \cdot \sqrt{T} \cdot \exp(-25520/T)$ ;  $k_{2,1} = 10^{-4} T_e^{-0.67}$ ;  $k_{2,2} = 10^{-6}$ ;  $k_{2,3} = 10^{-9} \exp(-104400/T_e)$ ;  $k_{2,5} = 10^{-5} T_e^{-0.67}$ ;  $k_{3,3} = 10^{-3} \exp(-37120/T_e)$ ;  $k_{3,1} = 10^{10} \text{ s}^{-1}$ . Equilibrium parameters:  $[A_{2e}^+] = 10^{12} \text{ cm}^{-3}$ ,  $[A_e^+] = 7 \cdot 10^{13} \text{ cm}^{-3}$ .  
 1) without regard for absorption of emanation by ions  $A_2^+$ ; 2) with regard for absorption of emanation;  $k_{1,4}^1 = 1.8 \cdot 10^7 \text{ s}^{-1}$ ,  $k_{1,4}^2 = 2 \cdot 10^6 \text{ s}^{-1}$ .

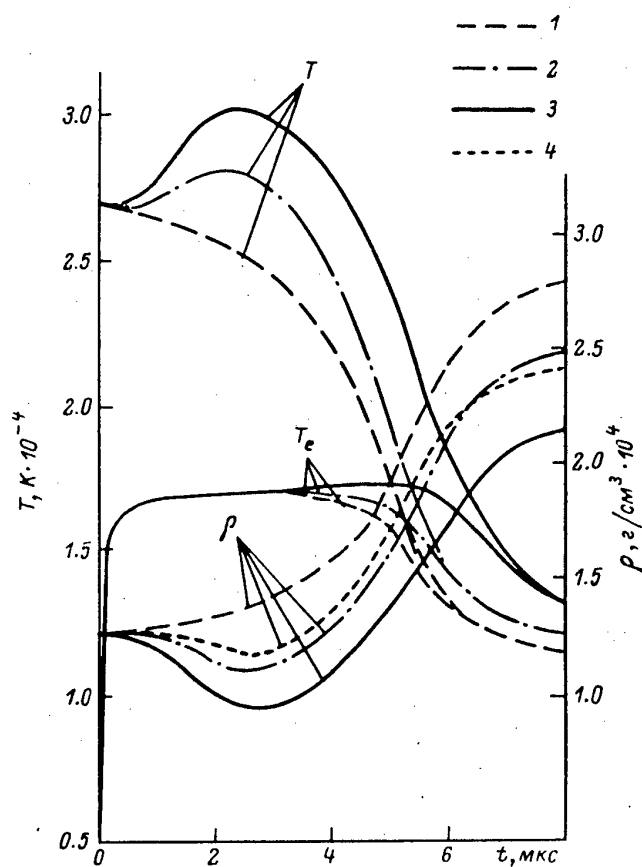


Fig.10. Distribution of gasdynamic parameters and  $T_e$  behind shock front in Xe (parameters before front are the same as on Fig.9) [29]: 1) without regard for absorption of emanation by ions  $\text{Xe}_2^+$ ; 2)  $k_{1.4}^j = 9 \cdot 10^6 \text{ s}^{-1}$ ,  $k_{1.4}^i = 10^6 \text{ s}^{-1}$ ; 3)  $k_{1.4}^j = 1.8 \cdot 10^7 \text{ s}^{-1}$ ,  $k_{1.4}^i = 2 \cdot 10^6 \text{ s}^{-1}$ ; 4)  $k_{1.4}^j = 1.4 \cdot 10^7 \text{ s}^{-1}$ ,  $k_{1.4}^i = 6 \cdot 10^6 \text{ s}^{-1}$ . 2-4) with regard for emanation absorption,  $J(\Delta\lambda) = 10^4 - 2 \cdot 10^4 \text{ Wt/cm}^2$  in field  $\Delta\lambda = 200 - 500 \text{ nm}$ .



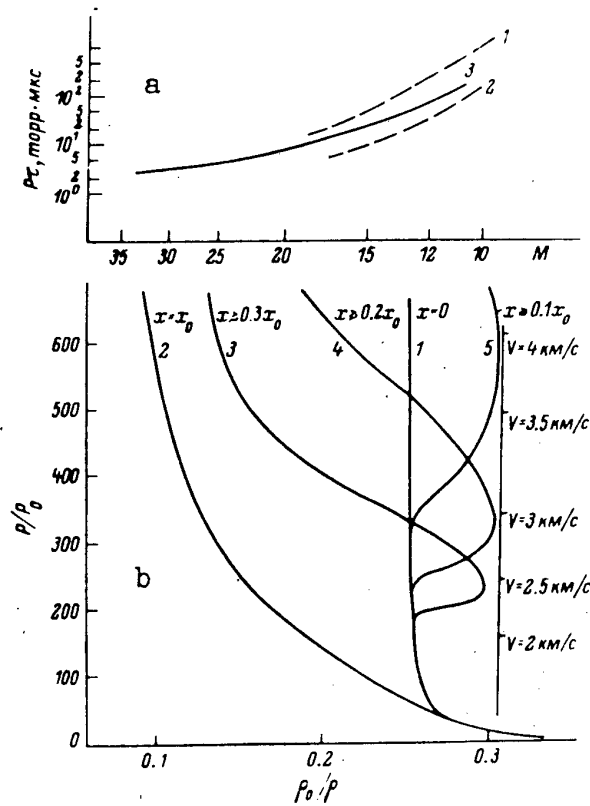


Fig.11. a) Dependence  $p\tau$  on  $M$  ( $p$ -pressure before shock,  $\tau$ -relaxation time):  
 1) experiment [66]; 2) experiment [67]; 3) calculation [30].  
 b) Hugoniot's adiabat for states behind shock wave in Xe ( $p_1 = 5 \text{ Torr}$ ,  $T_1 = 300 \text{ K}$ ): 1- equilibrium state, 2) frozen state; 3-5) nonequilibrium state.  
 $V = 4 \text{ km/s}$ ;  $x_0 = 0.5 \text{ cm}$ ;  $V = 2 \text{ km/s}$ ;  $x_0 = 4 \text{ cm}$  ( $x_0$  - length of relaxation zone).

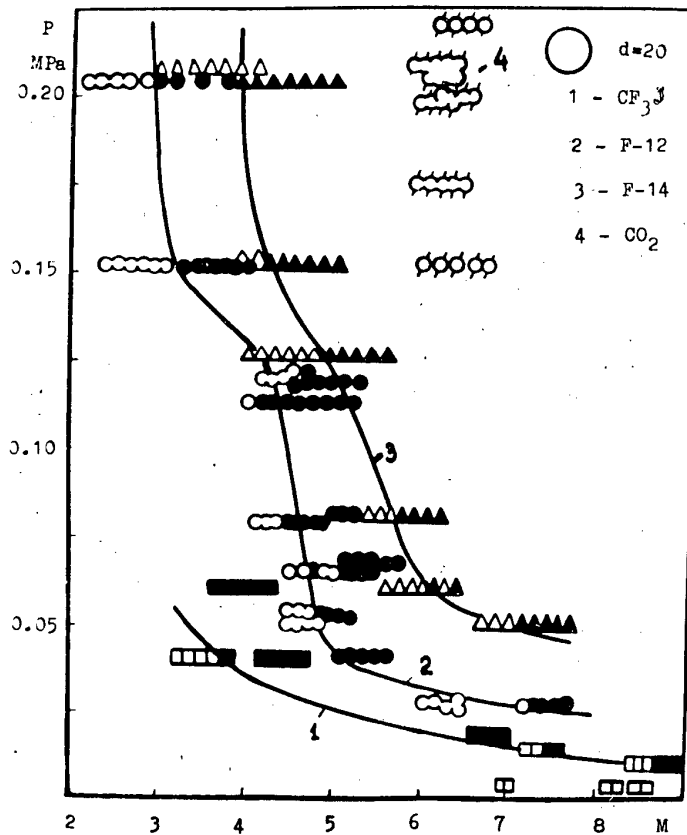


Fig.12. Neutral curves  $p = p(M)$  for the sphere in different gases. Dark points: flow is unstable, light points: flow is steady.

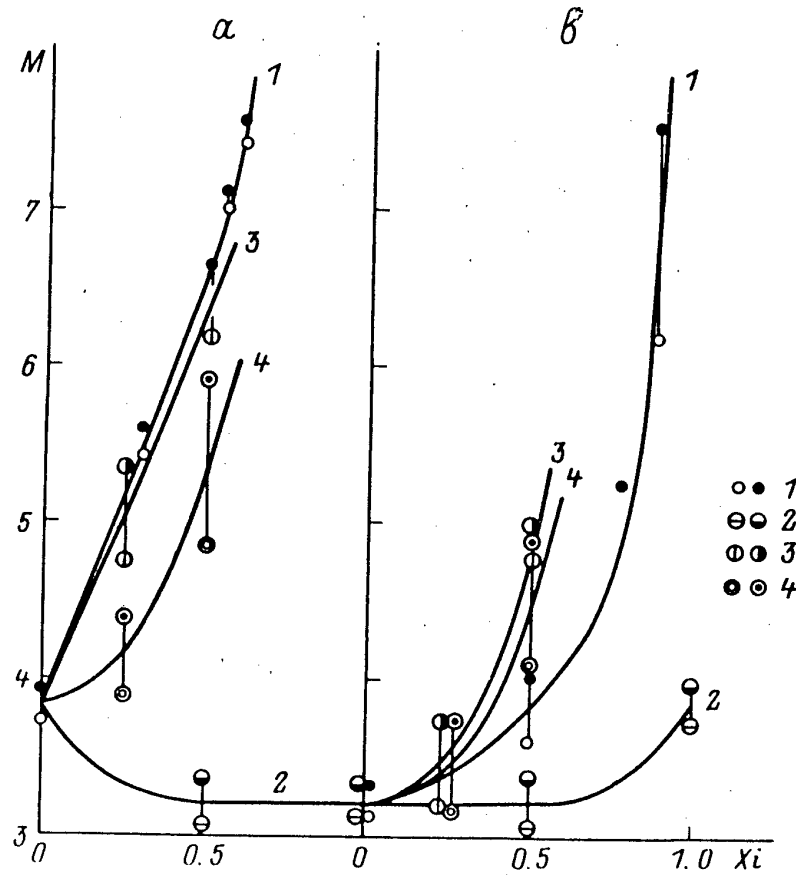


Fig.13. Neutral curves  $M=M(x_i)$  for segmental body ( $d=27\text{mm}$ ,  $R/d=1.5$ ) in freons-12, 114 and their mixture with inert gases:  
 a) freon-12 and its mixture: 1) F-12; 2) F-12+F-114; 3) F-12+Ar; 4) F-12+Xe;  
 b) freon-114 and its mixture: 1) F-114; 2) F-114+F-12; 3) F-114+Ar; 4) F-114+Xe;  
 $x_i = p_i / p$ ,  $p = 0.04\text{MPa}$  is mixture pressure,  $p_i$  is partial pressure of admixture,  $p_{\text{F12,114}} = 0.04(1-x_i)$  MPa is pressure in pure freons.

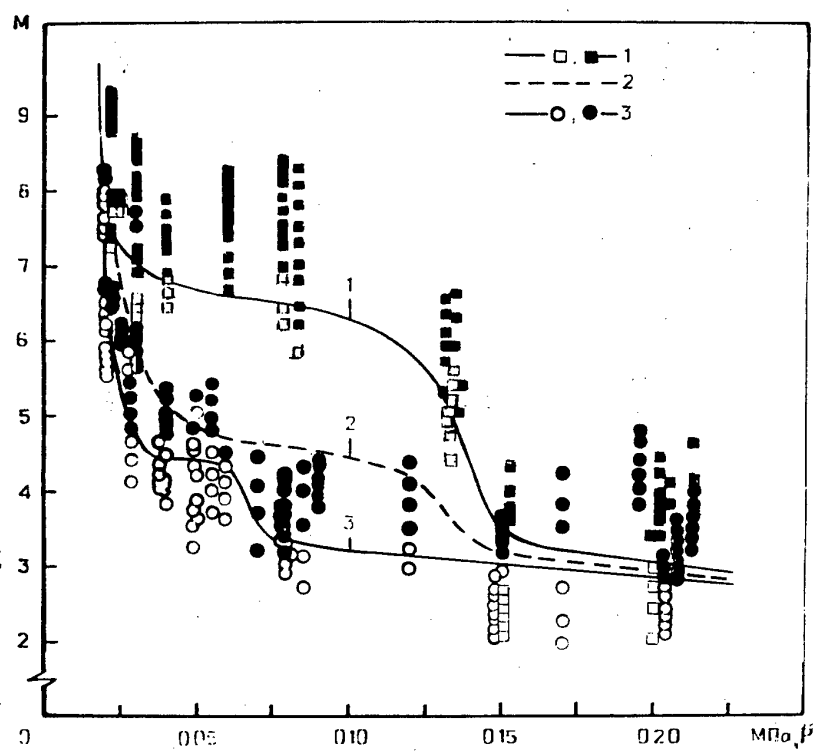


Fig. 14. Neutral curves in freon-12 for sphere of different diameters  $d$ : 1) 10mm, 2) 20mm, 3) 27. Dark points: flow is unsteady; light points: flow is steady.

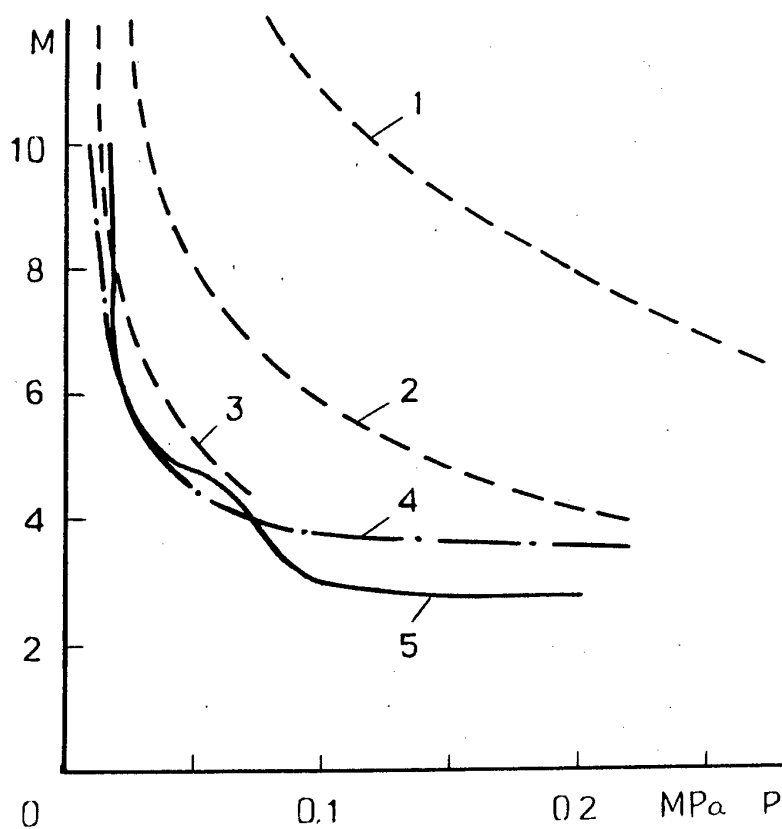


Fig.15. Neutral curves in freon-12 for different bodies ( $d=27\text{mm}$ )[33].  
 Calculation: cone, angle: 1)  $30^\circ$ ; 2)  $60^\circ$ ; 3)  $120^\circ$ ; experiment: 4) segment body ( $R/d=1.5$ ); 5) sphere.



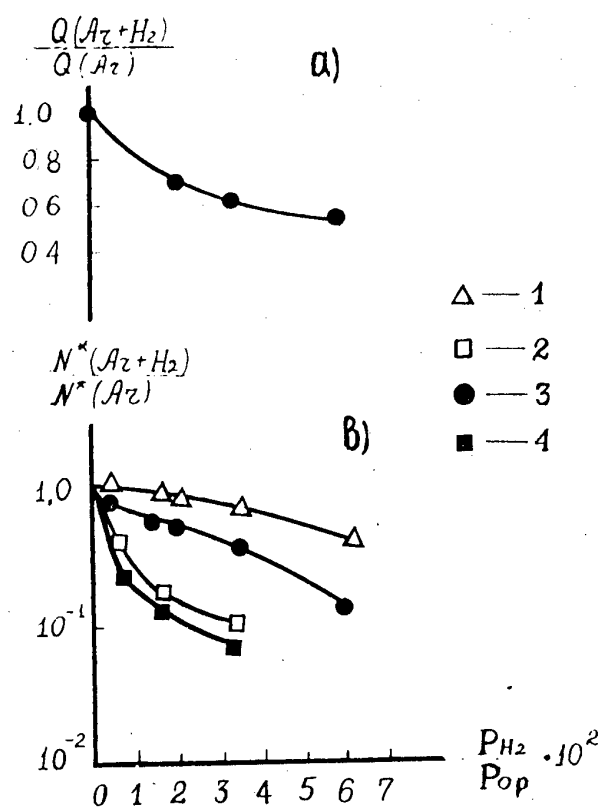


Fig. 18.  $H_2$  admixture influence on heat flux (a) and on Ar excited atom concentration in shock wave (b).

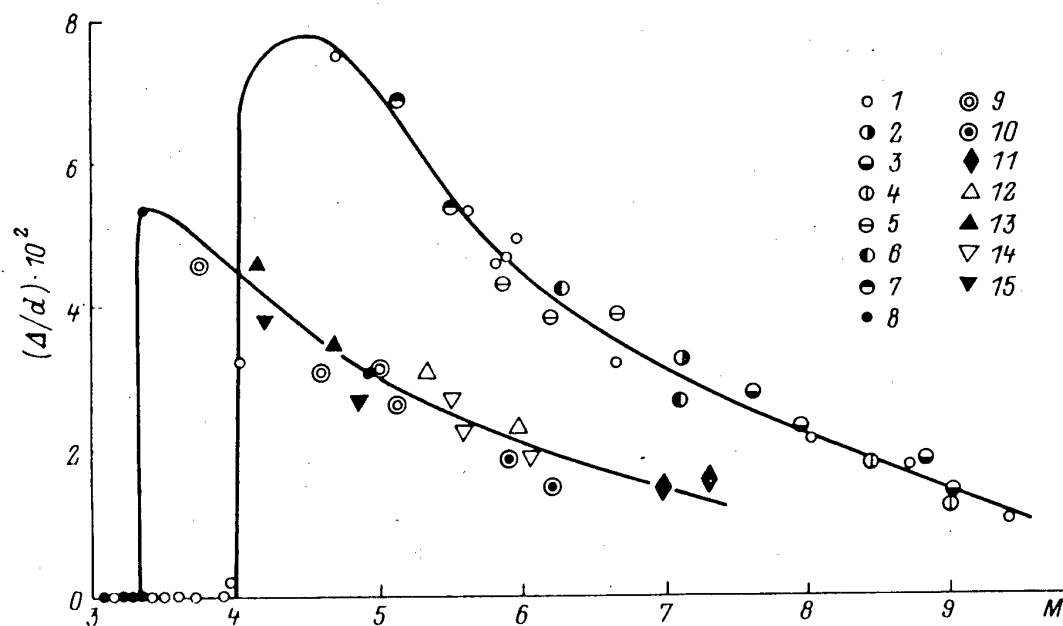


Fig. 19. Relative amplitude of pulses of bow shock wave detached from segmental body ( $R/d=1.5$ ,  $d=27$ )  $\Delta/d$  versus number  $M$  in freons and their mixtures. F-12,  $p$ : 1) 0.04 MPa; 2) 0.03; 3) 0.017; 4) 0.012; mixtures,  $p=0.04$  MPa: 5) 0.75F-12+0.25Ar, 6) 0.5F-12+0.5Xe; 7) 0.75F-12+0.25Xe; F-114,  $p$ : 8) 0.04 MPa; 9) 0.02; 10) 0.01; 11) 0.005; mixtures,  $p=0.04$  MPa: 12) 0.5F-114+0.5Ar, 13) 0.75F-114+0.25Ar, 14) 0.5F-114+0.5Xe; 15) 0.75F-114+0.25Xe.



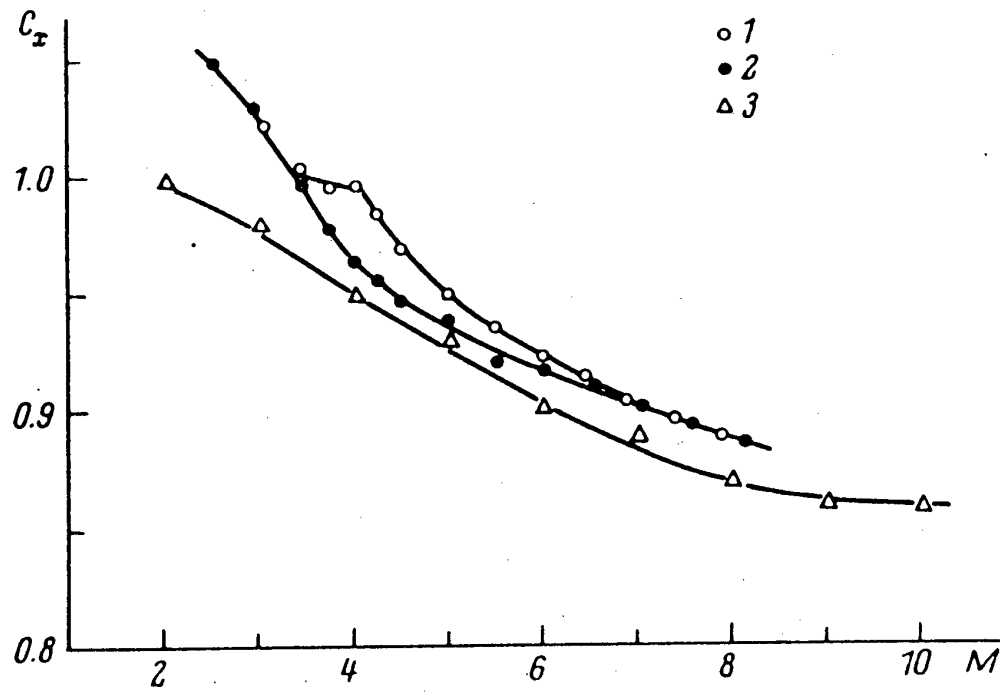


Fig.20. Drag coefficient of sphere in freon-12 and air versus number  $M$ .  
 Freon-12: 1)  $Re = 1.5 \cdot 10^7$ , 2)  $2 \cdot 10^6$  [23]; air: 3)  $Re > 2 \cdot 10^6$  [68].

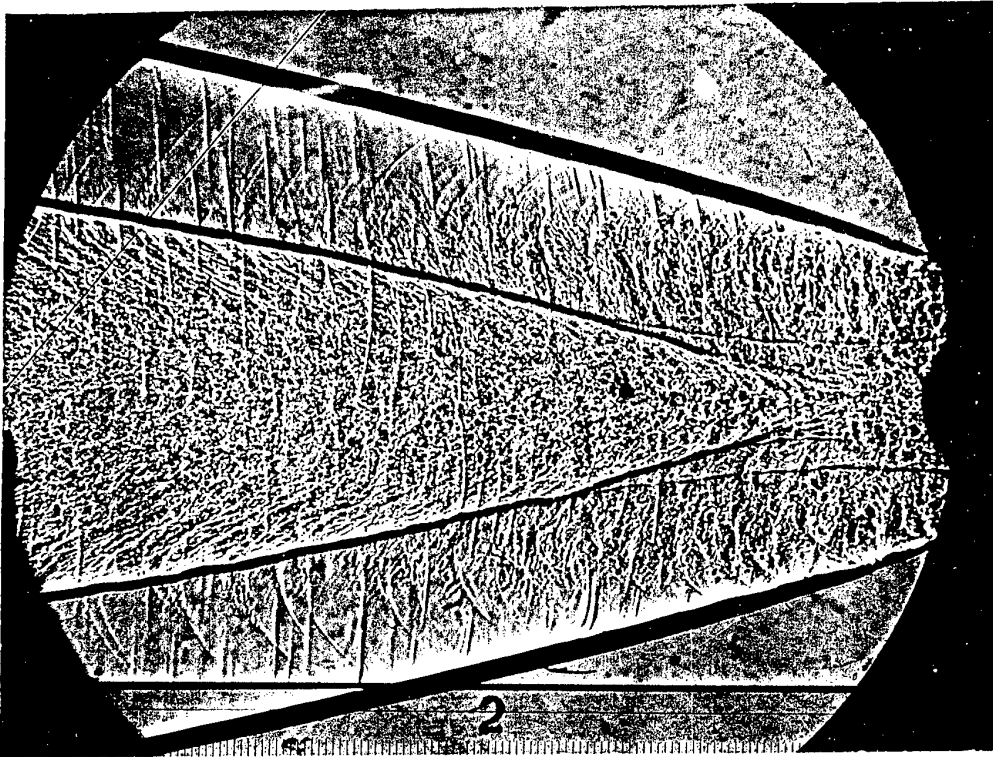


Fig.21. Fir-structure of wake.

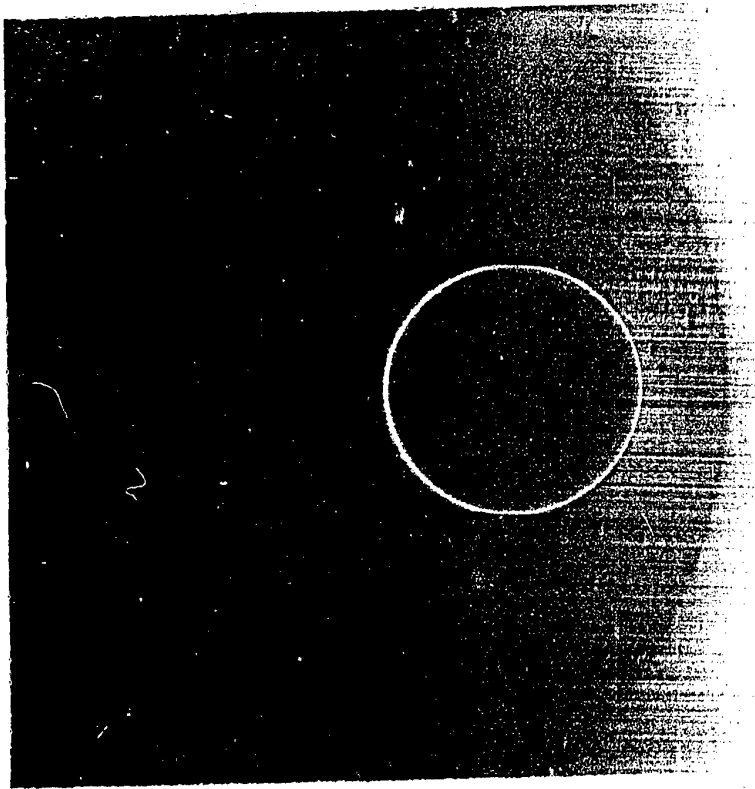


Fig.22. Flow around sphere in air plasma [46,47].  $V=2100\text{m/s}$ ;  $d=20\text{mm}$ ; plasma pressure is 40 Torr, its temperature is  $\sim 1400\text{K}$  [46,47].

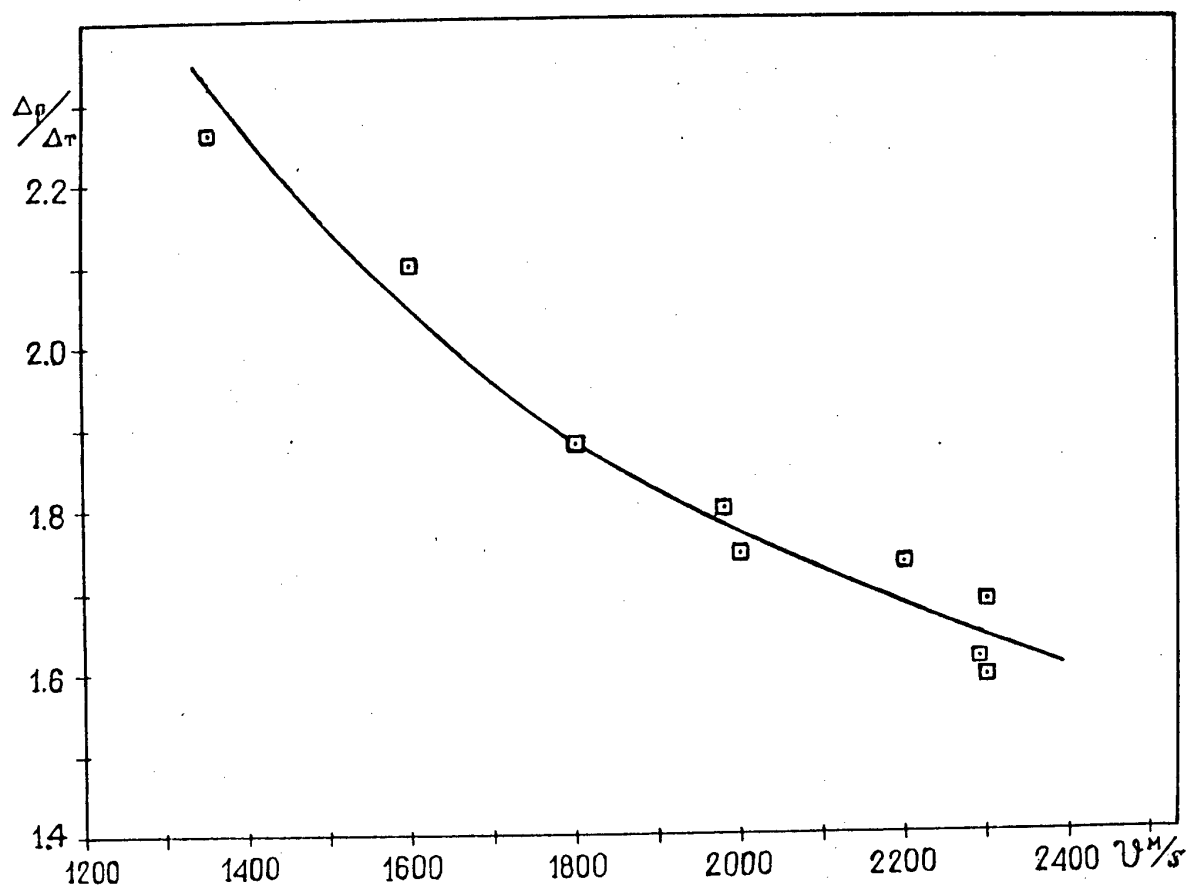


Fig.23. Ratio of the detachment of shock wave from sphere in plasma  $\Delta_p$  to the same in heated air  $\Delta_\tau$  versus model velocity [46,47].

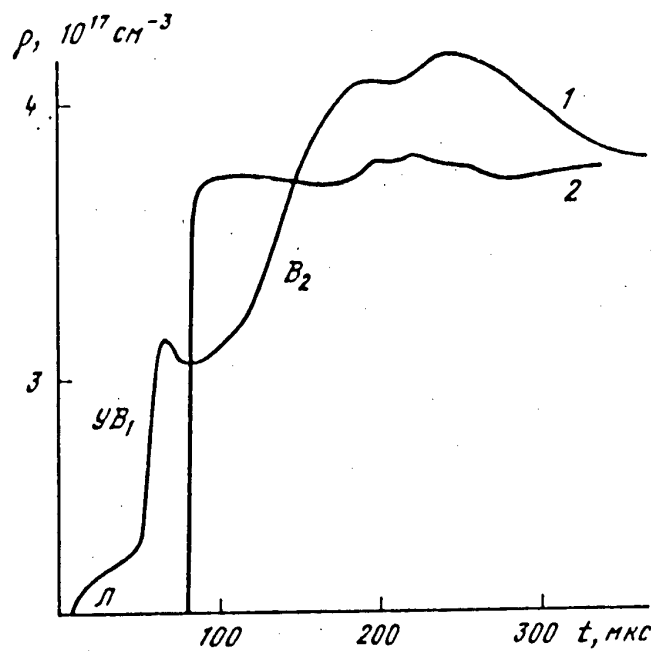


Fig.24. Density behind shock wave ( $V=500\text{m/s}$ ) in: 1)plasma; 2)cold air [39].

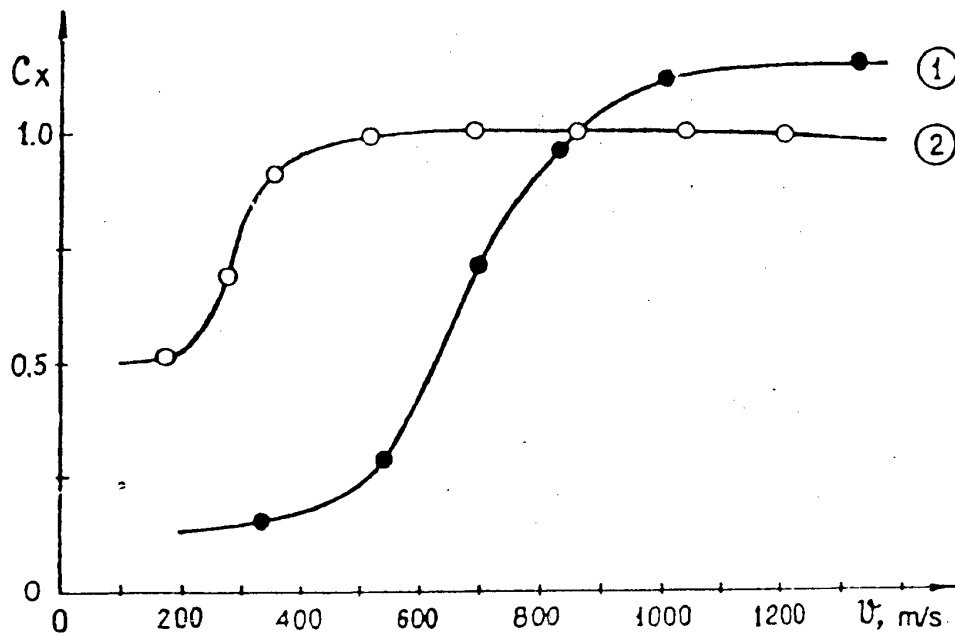


Fig.25. Coefficient  $C_x$  of sphere versus its flight velocity  $V$  in: 1)plasma; 2)cold air. Temperature of plasma is  $\sim 1250\text{K}$ , pressure is 15Torr, diameter of sphere is 15mm.

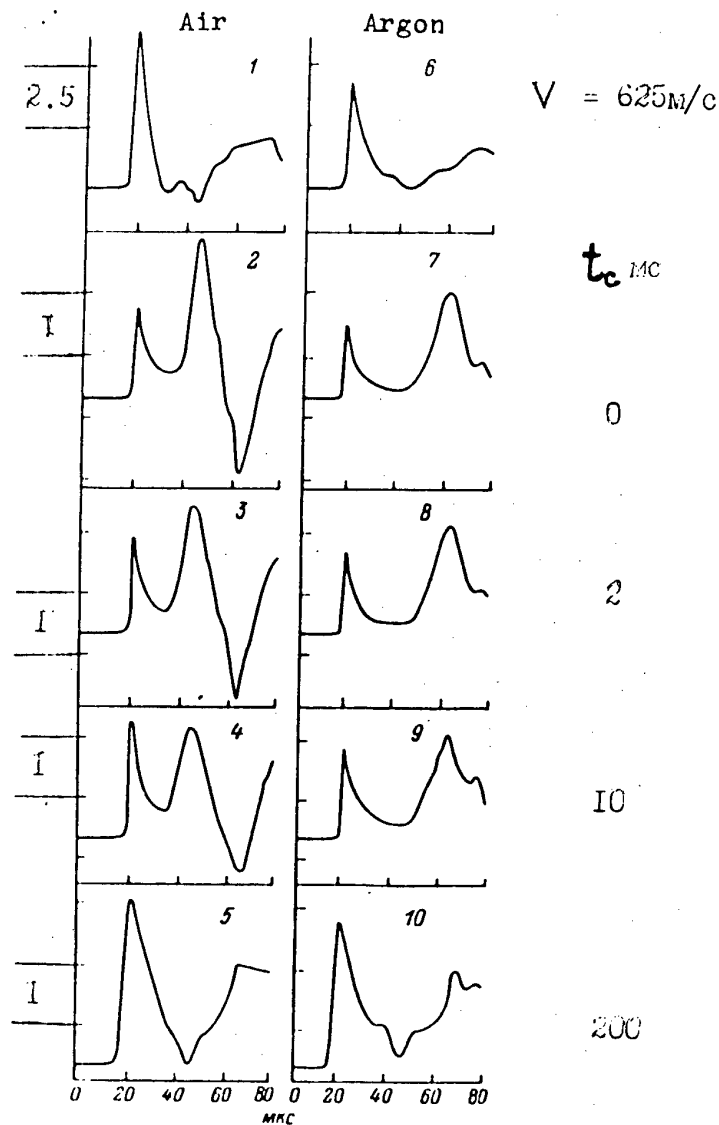


Fig.26. Character of change of pressure in centre of decaying plasma of air (2-5) and of Ar (7-10) when moving shocks through glow discharge in different intervals of time after current interruption  $t_c$ : 1,2-air and Ar without ionization ( $p=33 \text{ Torr}$ ,  $T=293 \text{ K}$ ). Temperature of plasma is  $1420 \text{ K}$  in air and  $1000 \text{ K}$  in Ar.

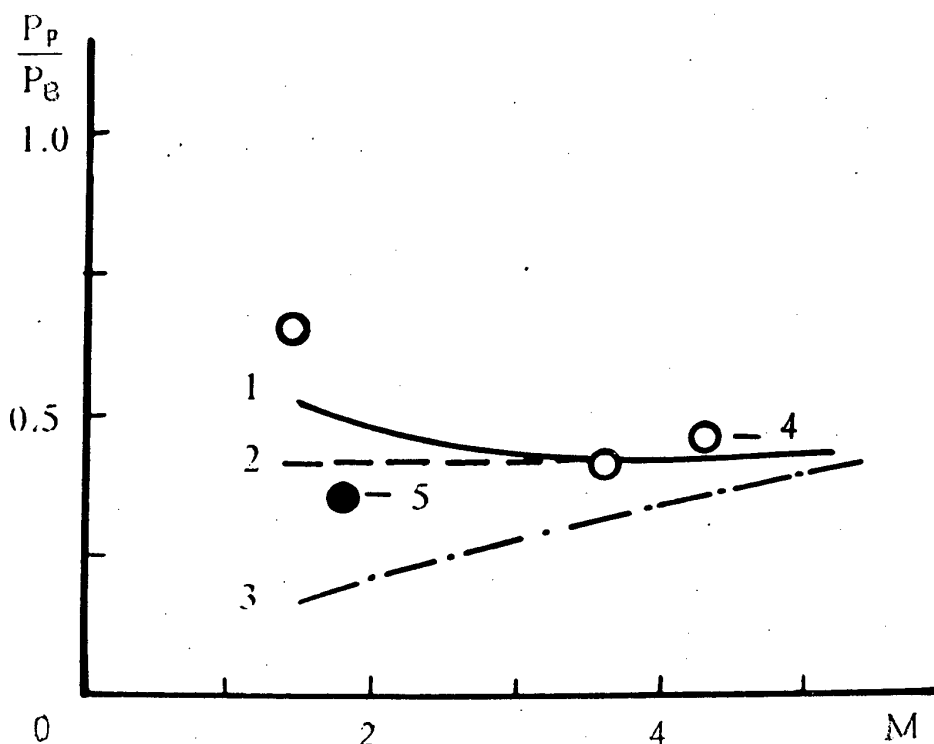


Fig. 27. Ratio  $p_p/p_g$  ( $p_p$  is pressure behind precursor in plasma,  $p_g$  is pressure behind shock wave in air) as a function of number  $M$ . Calculation [49]: 1) static pressure, 2) stagnation pressure, 3) pressure behind shock wave reflected on flat wall; experiment: 4) [39,40]; 5) [51].

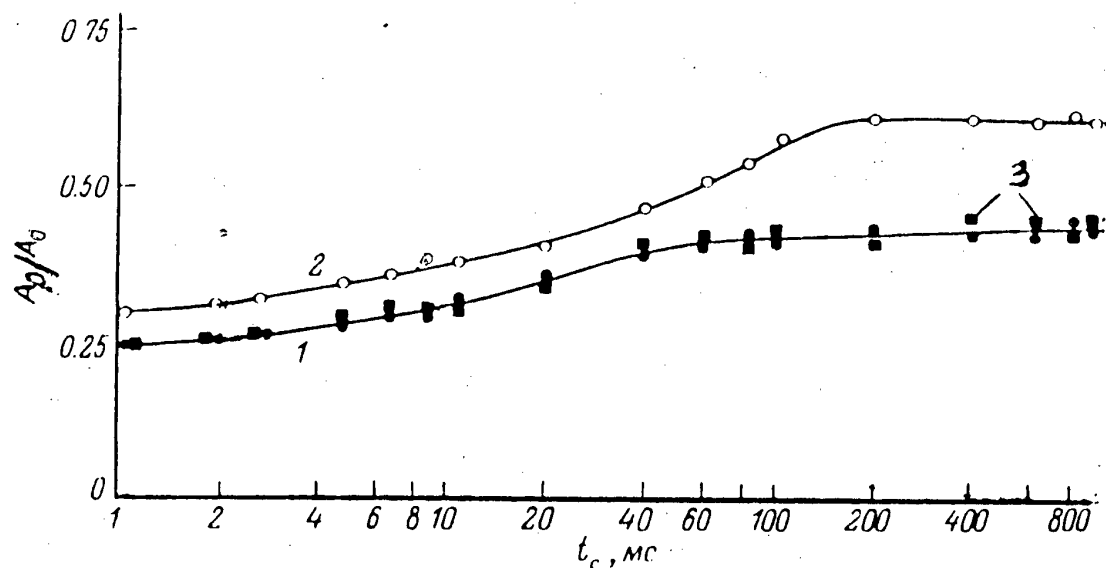


Fig. 28. Character of change of relative amplitude of precursor in decaying plasma of air (1), Ar (2) and mixture 0.1Ar+0.9air (3).  $A_p, A_0$  are amplitudes of precursor in plasma and shock wave in nonionized gases.

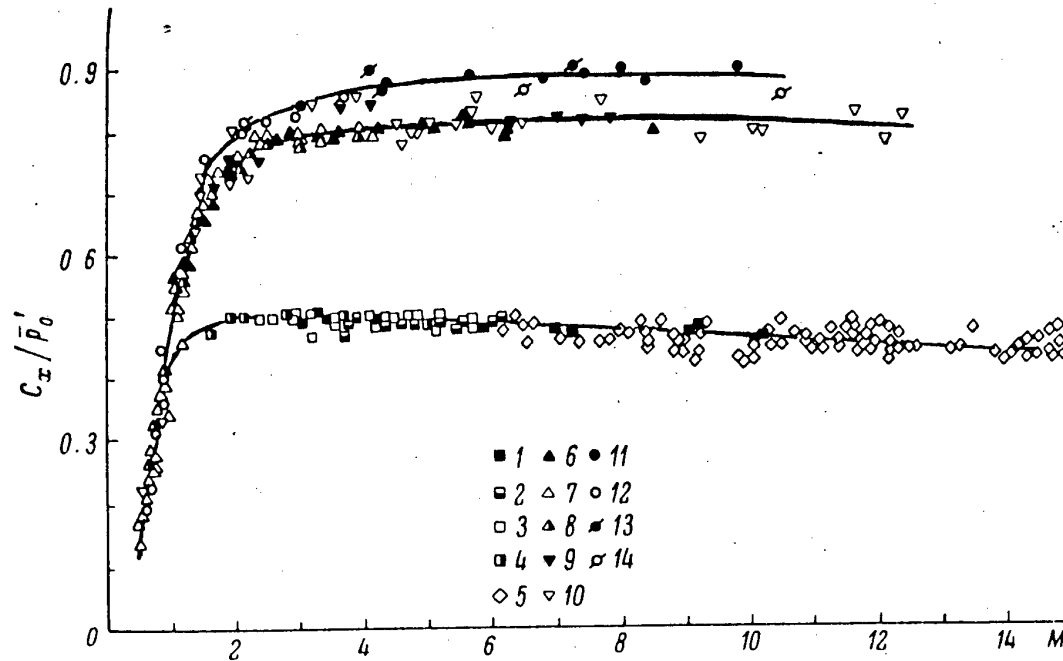


Fig. 29. Generalizing of results of measurement of drag coefficient of blunted bodies in different gases.

Sphere,  $\gamma$ : 1)1.14, 2)1.29, 3)1.41, 4)1.67[69,70]; 5)1.41[68];

segment ( $\theta_c=60^\circ$ ),  $\gamma$ : 6)1.14, 7)1.41, 8)1.67[4];

blunted cone ( $\theta_c=60^\circ$ ),  $\gamma$ : 9)1.16, 10)1.14 [71];

segment ( $\theta_c=70^\circ$ ),  $\gamma$ : 11)1.14, 12)1.41[4];

blunted cone ( $\theta_c=70^\circ$ ),  $\gamma$ : 13)1.16, 14)1.41[71].



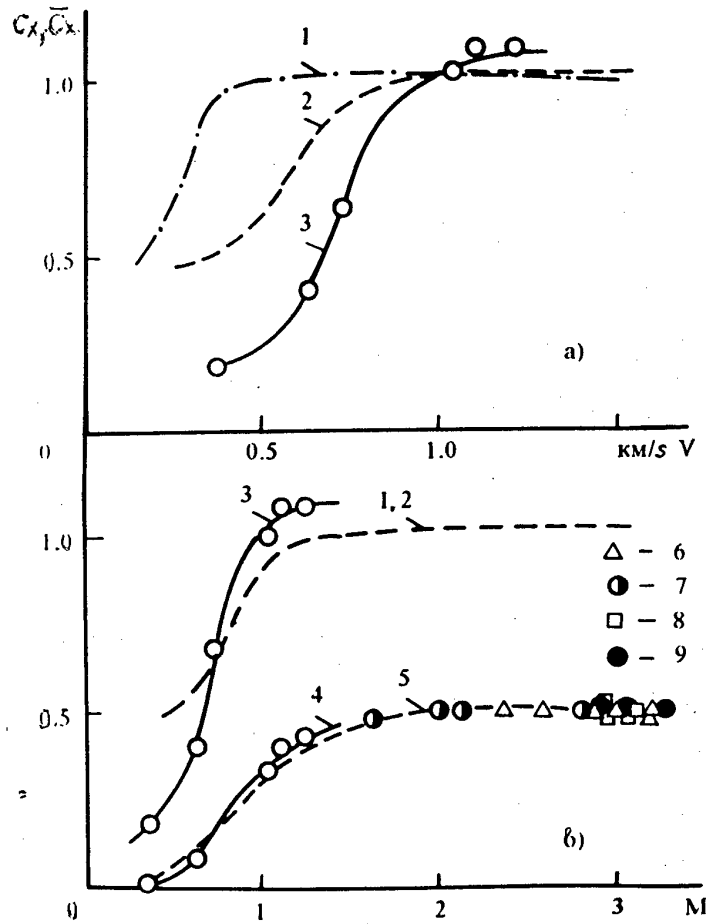


Fig.30. Drag coefficients of sphere  $C_x$  and  $\bar{C}_x = C_x / \bar{p}_0$  ( $\bar{p}_0 = 2p'_0 / \rho V^2$ ) in different mediums:

$C_x$ ,  $p=2kPa$ : 1)air ( $T=290K$ ); 2)air ( $T=1250K$ ); air plasma ( $T=1250K$ );

$\bar{C}_x$ ,  $p=2kPa$ : 4)air plasma, 5)air;

$p=0.1MPa$ : 6)air, 7) $CO_2$ , 8)Ar, 9)  $CF_2Cl_2$ .

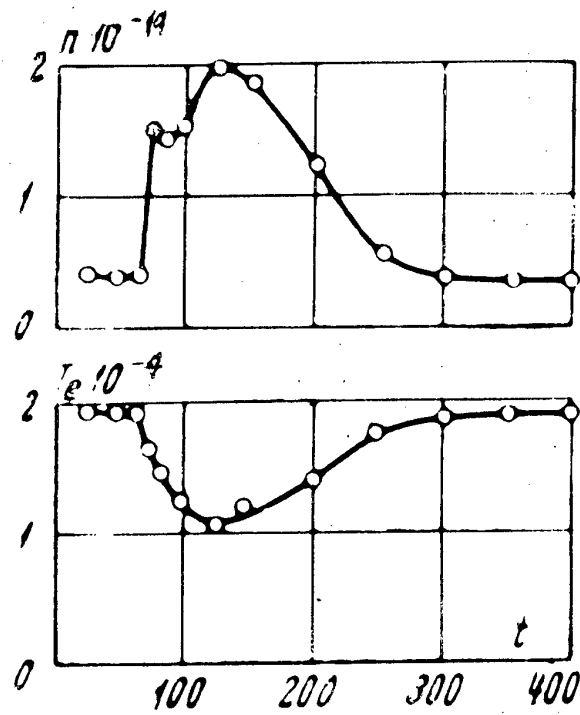


Fig.31. Concentrations of charged particles  $n$  and electron temperature  $T_e$  near shock front in argon plasma [56].

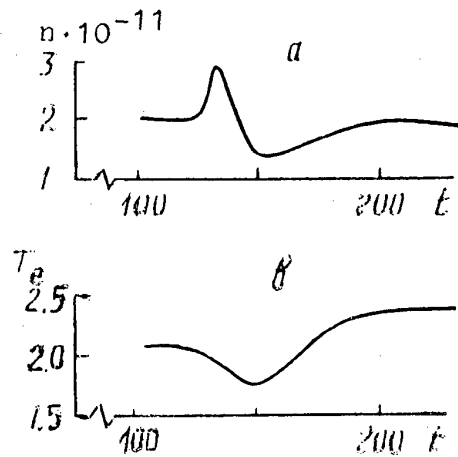


Fig.32. Concentrations of charged particles  $n$  and electron temperature  $T_e$  near shock front in nitrogen plasma [57].

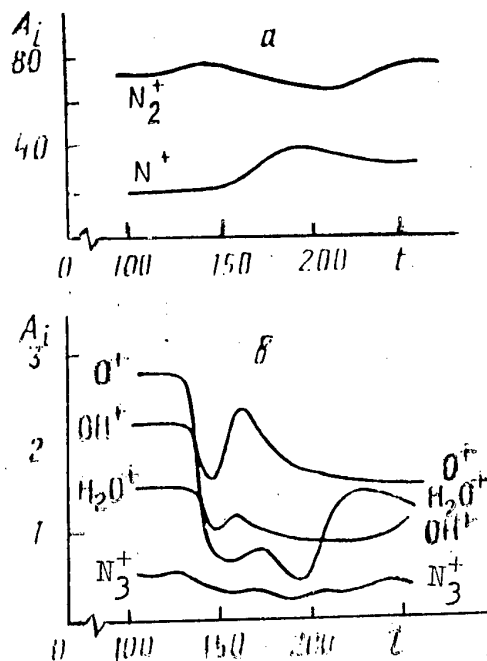


Fig.33. Ions concentration near front of shock wave in discharge nitrogen plasma [57],  $A_i$ , %.

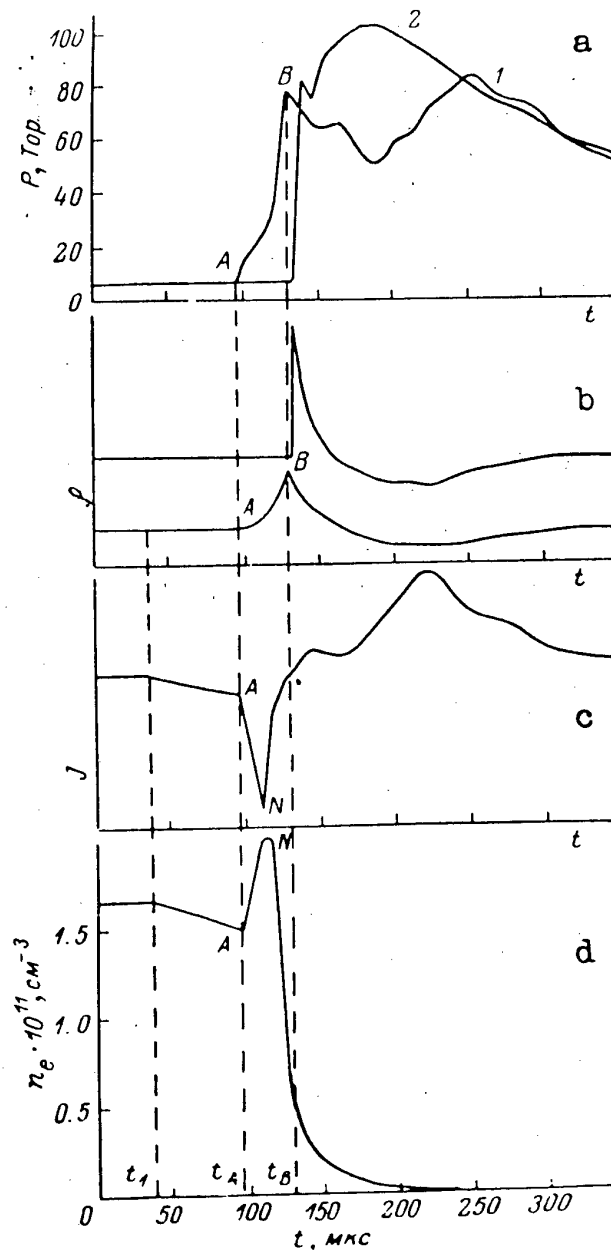


Fig.34. Character of change of pressure  $p$  (a), of density  $\rho$  (b), of plasma luminosity  $J$  (c) and of electron concentration  $n_e$  (d) with time during movement of shock wave in plasma (1) and in cold air (2).

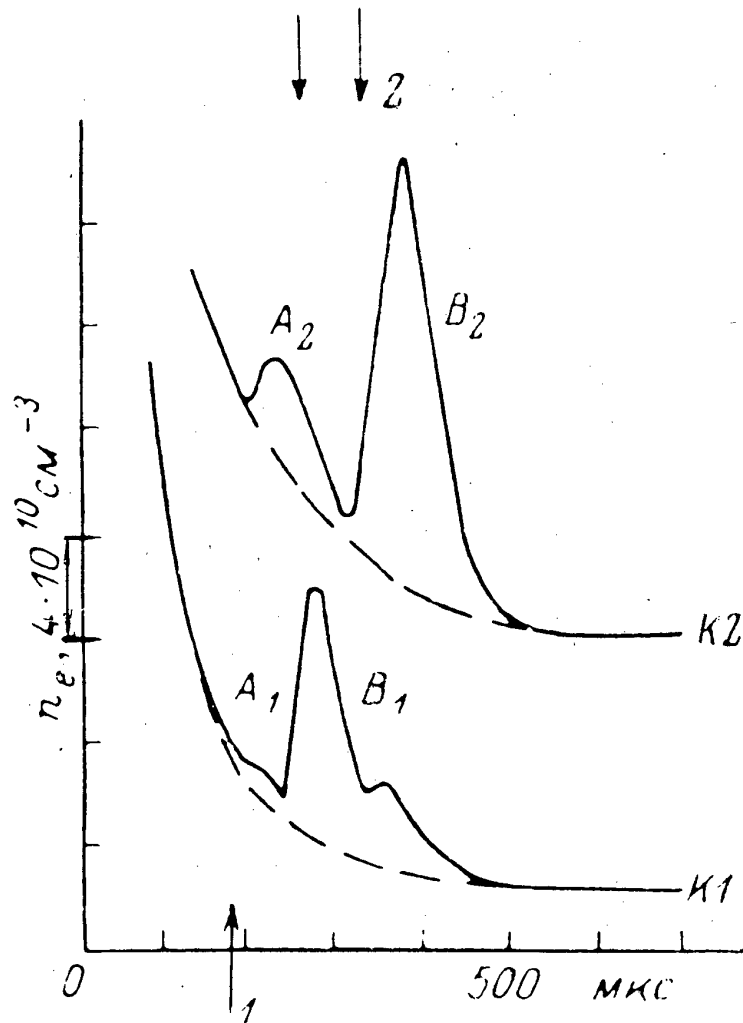


Fig.35. Oscillograms of SHF signals in  $\text{CO}_2$  plasma of pulse discharge :  
 1) moment of entrance of shock in discharge field;  
 2) time of coming of shock to section where two schlieren-systems are placed; A, B are maxima of  $n_e$ ; channels  $k_1$ ,  $k_2$  are placed 150mm one after another,  $p=6\text{Torr}$ ,  $V=1200\text{m/s}$ .

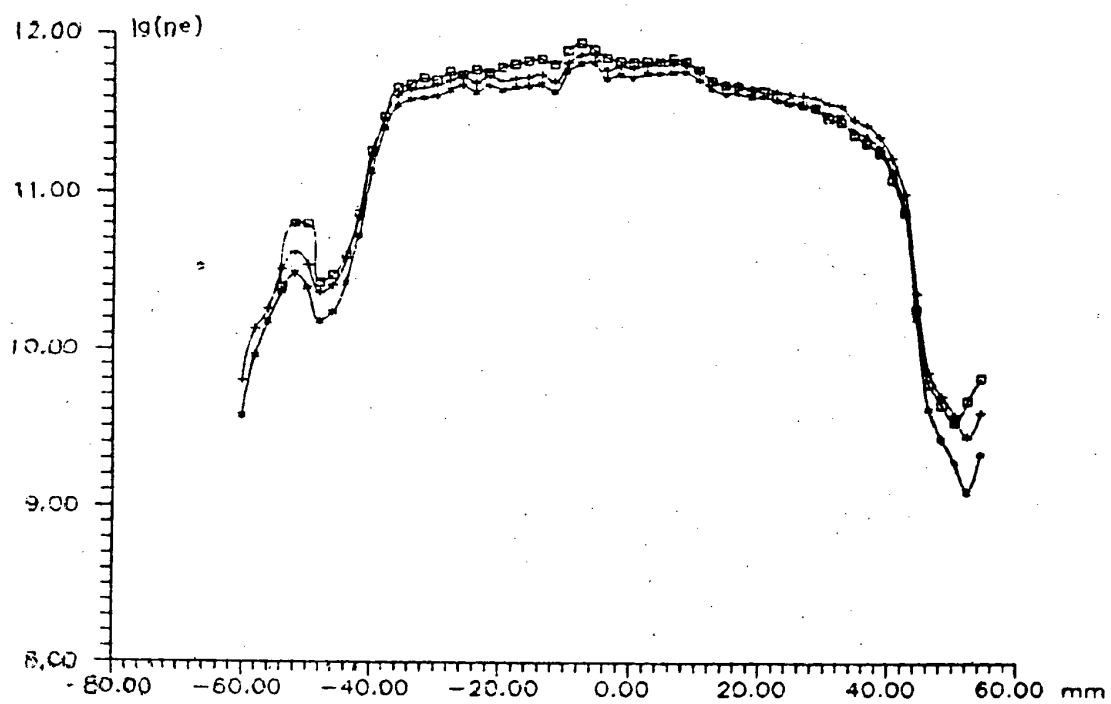


Fig.36. Radial distribution of electron concentration  $n_e$  in glow discharge. Data are obtained by 3 methods of treatment AV characteristics.

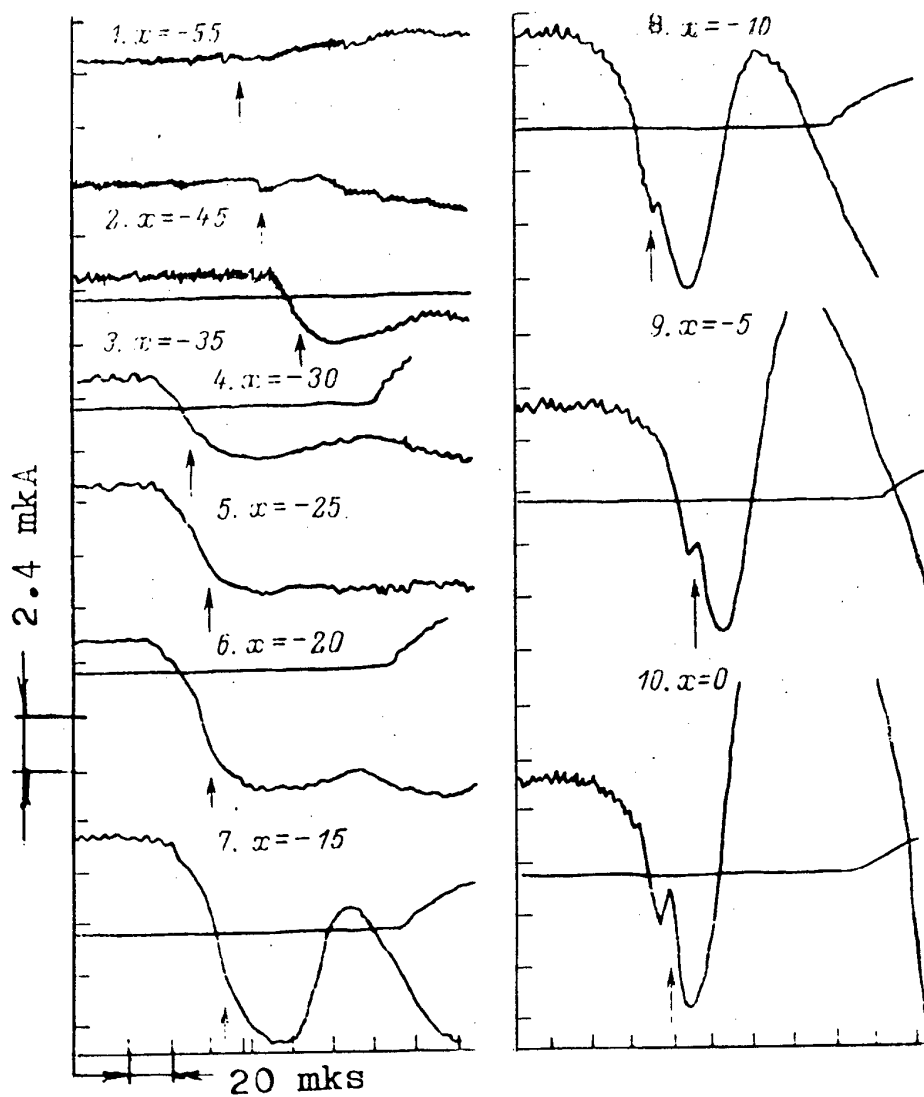


Fig.37. Oscillograms of current impulses of double probe:  $x$ - position of probe with respect on axis of discharge , mm; position of shock front is shown by arrow.

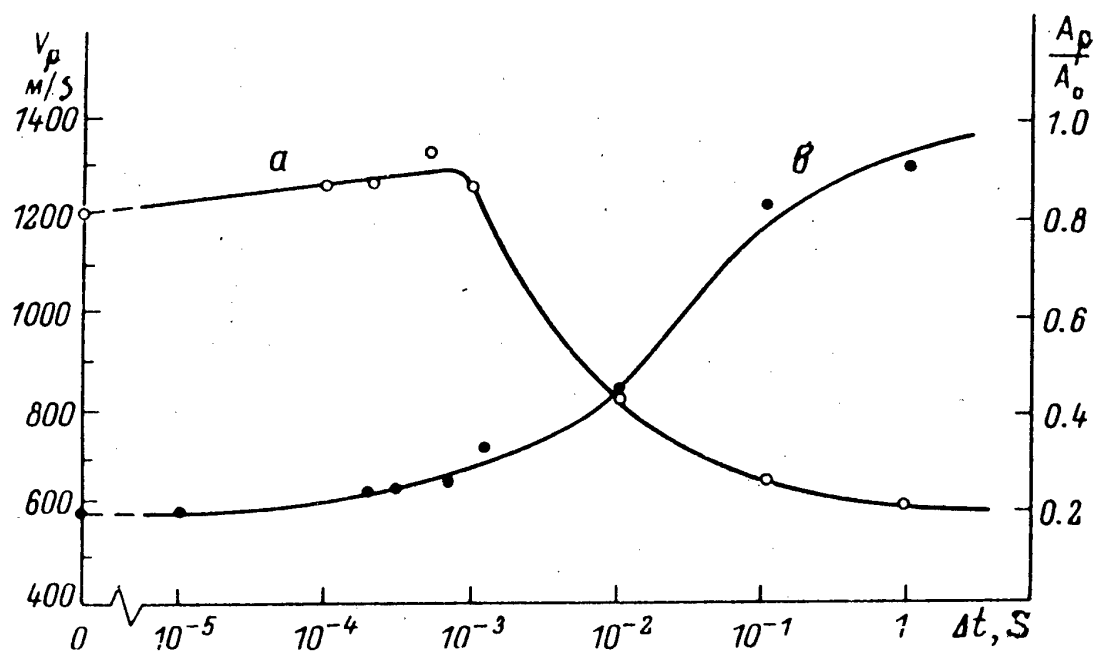


Fig.38. Dependences of velocity (a) and amplitude (b) of shock wave in decaying plasma on time.  $A_0$ ,  $A_p$  - amplitudes of shock wave in cold air and in plasma.



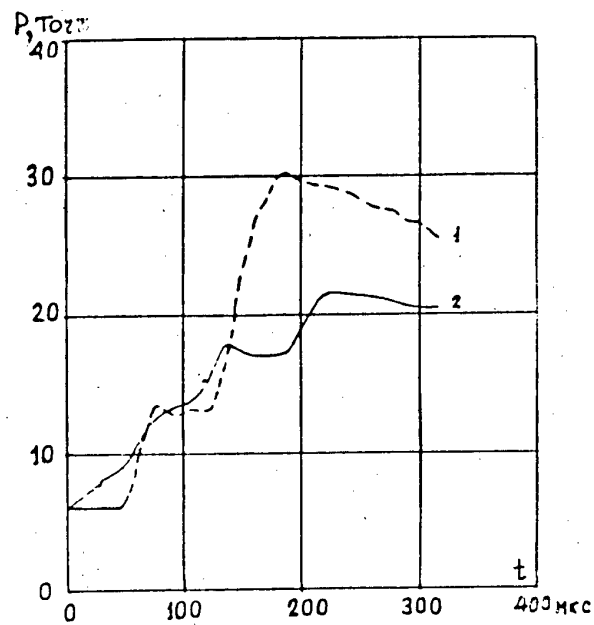
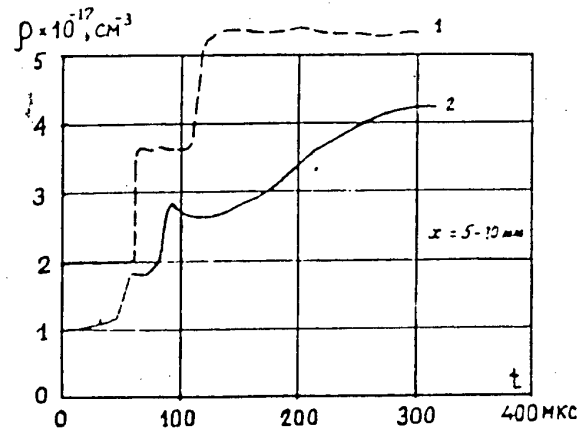


Fig.39. Structure of shock wave reflected from flat wall in cold air (1) and plasma (2).  $p=12\text{Torr}$ ,  $V=500\text{m/s}$ .